------- Iraqi National Journal of Earth Sciences, Vol. 13, No. 1, pp. 103 – 137, 2012-------

Pre-collisional Intrusive Magmatism in the Bulfat Complex, Wadi Rashid, Qala Deza, NE Iraq: Geochemical and Mineralogical Constraints and Implications for Tectonic Evolution of Granitoid-gabbro Suites

Khalid J. Aswad
Department of Geology
College of Science
University of Mosul

Ruaa M. Al.Sheraefy
Department of Geology
College of Science
University of Mosul

Sarmad A. Ali
Department of Applied Geology
College of Science
University of Kirkuk

(Received 2/9/2012 , Accepted 27/9/2012)

ABSTRACT

Pre-collisional plutonic rocks of Bulfat Complex, Qala Deza, NE Iraq were emplaced into the ophiolite-bearing terraine (Albian-Cenomenian) shortly after the 45Ma. At Wadi Rashid, the plutonic rocks consist of contemporaneous leucocratic 'granitoid' and melanocratic 'gabbro' rock types, with a "Daly gap" (compositional bimodality) that spans ~50–60 wt% SiO_2. The relationship between the granitoid and gabbro magmas at Wadi Rashid in particular is ambiguous. This is attributed to rock types having their own geochemical characteristics. Reconnaissance data suggest that Wadi Rashid granitoid is illustrated by characteristics akin to a volcanic-arc granitoid setting. Their enrichment in the LREE relative to HREE is relatively modest (La/Yb ratios are 4.46-8.61× chondrite), with Eu anomalies that are typically positive. The low HREE in Wadi Rashid granitoid rocks seems to be due to partial melting of metamorphosed oceanic crust leaving REE rich accessory minerals (i.e. garnet) as residual phases in the source. In contrast, the gabbros are all moderately light REE-enriched (La/Yb = ratios range from 1.77 to 3.43× chondrite), and flat heavy REE profiles (chondrite normalized Tb/Yb = ratios range from 1.09–1.28× chondrite) and small negative Eu anomalies (Eu/Eu*= 0.79-0.91). In primitive mantle-normalized multi-element diagrams, Wadi Rashid gabbroic samples show depletion in Pb and Sr relative to adjacent REE elements, Nb and Ta negative anomalies and flat Zr to Sm profiles similar to those of Enriched MORB. The Hf-Th-Ta, Nb-Zr-Y, Ti-Zr-Y and Ti-Zr-Sr diagrams of Wadi Rashid gabbros support an E-type MORB affinity. The geochemical data indicate that the gabbroic and granitoid rocks at Wadi Rashid are not cogenetically related. The dearth of intermediate magmatic compositions are

interpreted as the result of low to medium pressure breakup of pre-existing semi-consolidated and buoyant granitoid material due to density instabilities in the underlying crystal mush of the intruded gabbroic magma.

A puzzling aspect of Wadi Rashid granitoid- gabbroic suite is the variability of magmatic conditions (i.e. temperature, oxygen fugacity (fO_2) and water fugacity (fH_2O). Based on the empirical thermo-barometric results for kaersutite; The primary liquidus phases (i.e. augite, kaersutite and ilmenite) equilibrated at a nearly constant pressure of about 269-277 MPa and at temperatures of crystallization of about 933–935°C. $\log fO_2$ during equilibration of kaersutite in the hosting melanosome is in the range of -12.2 to -12.4 ($\Delta\log fO_2$ (FMQ) ~ 0.6). The petrography and mineral chemistry of leucocratic rocks indicate that there are two contrasting alkali metaluminous facies: (i) Fe-biotite granitoid and (ii) kaersutite-aenigmatite granitoid. These rocks occasionally encompass primary phases of mafic origin as resorbed xenocrysts (i.e. augite, An-rich plagioclase and ilmenite). Under such contrasting magmatic condition, primary ilmenite was transformed either into agpaitic (kaersutite-aenigmatite) or alkali metametaluminous (Ti-rich Fe-biotite) bearing mineral assemblages. These minerals are frequently observed in late-magmatic phase where the temperature of transformation of ilmenite ($\Delta\log fO_2$ (FMQ) ~ -4) into aenigmatite was about 753°C under H_2O^{melt} poor near-peralkaline conditions where as Ti-rich Fe-biotite equilibrated at about 647°C under H_2O^{melt} rich reducing conditions.

Wadi Rashid composite intrusion (Paleogene age) of arc affinity is unequivocally separated from the Walash-Naopurdan arc-backarc complex (Eocene– Oligocene); found in the same general area but in a structurally lower thrust slice. The Walash-Naopurdan volcanic activity and the intrusion of the multiphase Bulfat Complex indicate the presence of a dual subduction-zone system in Iraqi Zagros Zone.

Keywords: Zagros, Iraq, volcanic-arc granitoid, Collision zone, Bulfat Complex.

النشاطات الصهيرية الجوفية ما قبل التصادم القاري في معقد بلفات، وادي رشيد، قلعة دزا، شمال شرق العراق: المحددات الجيوكيميائية والمعدنية وآثارها على التطور التكتوني للمعية گرانيتود–گابرو

خالد جلال علي اسود
قسم علوم الأرض
كلية العلوم
جامعة الموصل

رؤى محمد حسن الشريفي
قسم علوم الأرض
كلية العلوم
جامعة الموصل

سرمد عاصي علي
قسم علوم الأرض
كلية العلوم
جامعة كركوك

الملخص

تموضعت الصخور الجوفية في معقد بلفات، وادي رشيد، قلعة دزا، شمال شرق العراق، في الاراضي الحاضنة للأفيولايت ophiolite-bearing terrene (البيان–سنومنيان). حدث التموضع قبل التصادم القاري(اي بعد ٤٥ مليون سنة). هنالك تنوع للصخور الجوفية في وادي رشيد في طبيعتها الصخارية منها الفاتحة leucocratic ' گرانيتود' و منها الداكنة melanocratic ' گابرو'، مع وجود "فجوة دالي" (ذات تركيبة ثنائية الموديل) وبمدى ~ ٥٠–٦٠ وزناً٪ من SiO_2. وتتسم العلاقة بين الصهارة الگرانيتودية والگابروية في وادي رشيد بالغموض.ويعزى هذا الغموض إلى احتفاظ كل نوع من هذه الصخور بخصائصه الجيوكيميائية. تشير البيانات الاستطلاعية إلى تميز گرانيتود وادي رشيد بعائديته الى تموضعات الگرانيتود للأقواس البركانية volcanic-arc granitoid. ومن أهم سمات صخور الگرانيتود هو الاغناء المتواضع نسبيا للعناصر الأرضية النادرة الخفيفة LREE نسبة إلى العناصر الأرضية النادرة الثقيلة HREE(نسبة La/Yb هي 4.46-8.61 × كوندريت)، مع شذوذ إيجابي لـ Eu . و يبدو أن قيم HREE منخفضة في الصخور الگرانيتود وينسب ذلك الانخفاض في هذه القيم (اي HREE) إلى الانصهار الجزئي للقشرة المحيطية الغائرة المتحولة تاركا المعادن الإضافية كأطوار متبقية في الجزء الصلب من المصدر المنصهر جزئيا والغنية بالعناصر الأرضية النادرة REE (مثل الگارنت). وفي مقابل ذلك، فإن مميزات صخور الگابرو لوداي رشيد هو اغناء متوسط لمجمل LREE (La/Yb= نسبة من ١.٧٧ إلى 3.43× كوندريت)، مع ملامح انبساط HREE (Tb/Yb المعير كوندرايتياً = 1.09حتي 1.28 × كوندريت) مع شذوذ سلبي صغير لى Eu (Eu/Eu*= 0.79-0.91). تظهر المخططات متعددة العناصر والمعايرة مع جبة بدائية primitive mantle، بان عينات الگابرو لوادي رشيد قد عانت استنزافا للىPb and Sr نسبة إلى العناصر الأرضية النادرة المجاورة لها، مع وجود شذوذ سلبي ملحوظ لـ Nb وTa و انبساط في النمط منZr الى Sm بذلك تشابه تلك الموجودة في مخططات بازلت حدبة أوسط المحيط الخصب (Enriched MORB). وهنالك دعم واضح من مخططات الفرز التكتوني Ti-Zr-Y وTi-Zr-Y وNb-Zr-Y و Hf-Th-Ta لعائدية گابرو وادي رشيد إلى EMORB. كما أكدت البيانات الجيوكيميائية المذكورة أعلاه وبشكل واضح بان صخور الگرانيتويد والگابرو في وادي رشيد ذات منشأ متباين. و تفسر ندرة الصخور ذات التركيب الصهيري المتوسط في المعية گرانيتود–گابرو granitoid-gabbro suites إلى التفكك الحاصل للمواد شبه المتصلبة لمكونات الگرانيتويد الطافي buoyant granitoid نتيجة لعدم استقرارها في كثافة عجينة البلورات العائدة للصهير الگابروي المقحم تحته .ومن مظاهر الحيرة لمعية الگرانيتويد– الگابرو وادي رشيد هو التباين الحاصل في ظروف الصهير(أي درجة الحرارة وهروبية الأوكسجين oxygen fugacity (fO_2) والماء water fugacity (fH_2O). و قد اتضح من نتائج مقاييس الحرارة والضغط thermo-barometric المستنبطة من التجارب المبنية على معدن الكيرسوتايت بان الأطوار الأولية وهي(augite, kaersutite ilmenite) كانت في حالة

توازن مع بعضها البعض عند ضغط ثابت تقريبا من حوالي ٢٦٩-٢٧٧ ميكا باسكال وعند درجة حرارة تبلور حول ٩٣٣-٩٣٥ درجة سليزية و تتأرجح قيمة هروبية الأوكسجين $\log fO_2$ المستحصلة من توازن kaersutite مع المعادن في الصخور الداكنة والمضيفة لها من 12.2- إلى 12.4- ($\Delta \log fO2$ (FMQ) ~ 0.6).

تشير الدراسة البتروغرافية وكيميائية المعادنmineral chemistry للصخور الفاتحة إلى وجود سحنتين متباينتين في سحنات متوسطة الالومينيا القلوية (alkali metaluminous facies) اولا: الكرانيتويد الغني بالبايوتايت الحديدي (Fe-biotite) ثانيا: كيرسوتايت-انيگميتايت -kaersutite aenigmatite و تحتضن الصخور المذكورة أحيانا أطوار أولية مافية الأصل وبشكل بلورات دخيلة xenocrysts متاكلة الحافات resorbed (الاوگايت والبلاجيوكليس الغني بالانوثايت والالمينايت). تحت مثل هذه الظروف المگماتية التي تتسم بالتناقض، يتحول الالمينايت الاولي إما إلى تجمعات معدنية االگبيتكية agpaitic (كيرسوتايت-انيگميتايت) أو تجمعات معدنية متوسطة الالومينيا القلوية (مثال: البايوتايت الحديدي والغني بالتيتنيوم). ويلاحظ وجود هذه المعادن في مرحلة صهيرية متأخرة ودرجة حرارة نسبيا منخفظة حيث ان تحول إلمينايت ilmenite ($\Delta \log fO_2$ (FMQ) ~ -4) إلى انيگميتايت aenigmatite كان في حوالي ٧٥٣ درجة سليزية مع شحة H_2O^{melt} في ظل ظروف تقترب من فوق القلوية peralkaline أما البايوتايت الحديدي Fe-biotite الغني بالتيتنيوم فانه يتبلور في حوالي ٦٤٧ درجة سليزية وفي ظل ظروف اختزالية وكذلك غنية بال H_2O^{melt}.

يتسم مقحم وادي رشيد (العمر الباليوجيني) بملامح قوس بركاني وينفصل و بشكل بين عن معقدات ولاش – ناوبردان ذات بيئة قوس- ظهر القوس البركاني Eocene arc-backarc) Oligocene) والمتواجدة في نفس المنطقة تقريبا ولكن في الشريحة الزاحفة السفلى. ويشير النشاط البركاني لولاش-ناوبردان ومقحمات متعدد المراحل لمعقد بلفات إلى وجود منظومة غورانية مزدوجة dual subduction في منطقة زاگروس العراقي.

الكلمات الدالة: زاگروس، العراق، الگرانيتود للأقواس البركانية، نطاق التصادم، معقد بلفات.

INTRODUCTION

Jabal Bulfat, 30 km east of Qala Deza City, NE Iraq, is a deeply dissected mountainous area composed generally of a wide spectrum of igneous rocks referred to as the Bulfat Complex (Jassim *et al.,* 2006). It forms a major part of the Upper Allochthon 'ophiolite-bearing terraine' and encompasses a volcano-sedimentary unit – the 'Gemo-Qandil Sequence'. This sequence was originally referred to the Bulfat Group by(Jassim *et al.*, 1982).This has been intruded by voluminous gabbro-diorite intrusions and late stage differentiates of syenite and nepheline syenite, forming epizonal multiphase intrusive bodies during an early Tertiary (Paleocene-Eocene) magmatic episode (Jassim *et al.,* 2006; Fig. 1).

The Gemo-Qandil Sequence has experienced a medium-grade regional metamorphism overprinted by a high-grade contact metamorphism during Paleogene (Jassim *et al.,* 2006).

Contact metamorphic rocks occur on the highest summits (~2340 m) forming roof pendants surrounding intrusions that protrude into this sequence (Buda, 1993). The pyroxene hornblende gabbros and diorites form a considerable part of the complex and generally contain calc-schist xenoliths. The dissemination of calc-schist xenoliths throughout the intrusion have resulted the from partial assimilation of Gemo-Qandil meta-sediment. In contrast, the metapelitic units of the meta-sediment have been completely assimilated; with only some streaks of biotite and relicts of the initial texture remaining. Peak temperature of the contact metamorphism of the calc-schist xenoliths is estimated to have been around 850°C corresponding to the pyroxene hornfels facies (i.e. calcite-melilite-diopside-anorthite assemblages). Most of the reactions occurred under low pressure and extremely water-deficient conditions (i.e. X_{CO2} ~0.9; Aswad and Pashdary, 1984). (Buda, 1993) suggested that the assimilation of the calcareous and pelitic host rocks resulted in peralkaline magma which led to the formation of pegmatite and nepheline syenite. (Jassim *et al.*, 2006) have noted that the calc-schist xenoliths are very rare in the olivine gabbro and diorite (i.e. younger intrusions) which are the least contaminated intrusions in the mafic Bulfat Complex. K-Ar dating of these rocks indicates a cooling age of 45 Ma, suggesting that the intrusions formed in the Paleogene and are, therefore, much younger than the Cretaceous country rocks (i.e. Gemo-Qandil Sequence; Jassim *et al.*, 2006).

It is unclear whether the pyroxene-hornblende gabbros and the diorites show geochemical and mineralogical constraints exclusively due to the assimilation of calcareous and pelitic host rocks by the mafic magma, or contamination of the magma with pre-existing granitoid rocks, or both. In view of this aspect, we undertook a combined in-situ mineral and whole-rock study of the gabbro along Wadi Rashid and its granitoid associate.

It is apparent from our in-situ field inspection that the studied igneous rocks within Bulfat Complex in Wadi Rashid near Pauza form a bimodal association, composed of leucocratic breccias within anatectic melt (granitoid; Fig. 2D) and melanocratic rockes (gabbro; Fig. 2B,C) forming a granitoid-gabbro suite. The melanosome–leucosome contact, however, is occasionally marked by an abrupt change in grain size and mineralogy, revealing the hybrid signature of the melanosome (Fig. 2D). The purpose of this paper is to describe the petrology, mineralogy and geochemistry of the granitoid rocks in Wadi Rashid and assess their impact on the gabbro intrusions. This will lead to an interpretation of the petrology and geotectonic evolution of the granitoid-gabbro suites in Wadi Rashid and to correlate them with the coeval Walash-Naopurdan arc-back arc volcanic rocks in the Lower Allochthonous thrust sheet.

GENERAL GEOLOGY

The nappe in the studied area, 30 km east Qala Deza City, NE Iraq, comprises allochthonous detachment of the Albian-Cenomanian Gemo-Qandil Sequence (Upper Allochthon) and the Paleocene-Eocene Walash Volcano-sedimentary Sequence (Lower Allochthon; Aswad *et al.,* 2011; Aziz *et al.,* 2011). On the basis of recent studies (Aziz *et al.,* 2011; Aswad *et al.,* 2011; Ali *et al.,* 2012), these two allochthonous sheets were juxtaposed and amalgamated into a single nappe (Walash-Penjween Subzone) following the closure of the Neo-Tethys. Coeval volcanic activity of Walash-Naopurdan 'Lower Allochthon' with the multiphase intrusion of the Bulfat Complex is common along the entire length of the Iraqi Zagros Suture Zone and the volcanic activity represents widespread arc-back arc volcanism during the Paleogene. With the exception of the Bulfat Complex, the remainder of the Lower Allochthon does not show any similar intrusive features. Furthermore, the thrust faults separating these two allochthons were formed due to later tectonic activity which presumably post-dates the emplacement of the Paleogene magmatic activity.

Field evidence shows that the nappe which incorporates the two amalgamated sheets rests on top of various units: Tertiary Mollasses (Tertiary Red Beds), Neoautochthonous flysch (Maastrichtian) and parautochthonous radiolarite (Albian-Cenomanian; Aswad, 1999). Exhumation of the Bulfat Complex occurred through the formation of nappes in a continental collision (Jassim and Buday, 2006) that terminated during the Middle Miocene (Aswad, 1999).

ANALYTICAL METHODS

Microprobe analyses were carried out on polished thin sections utilizing a fully automated, Cameca SX100 Electron Microprobe at Macquarie University, Australia, fitted with 5 wavelength dispersive spectrometers (WDS) and a PGT energy dispersive system (EDS). Further analytical details are provided by (Ali, 2012). Bulk whole rock chemical analysis of 12 samples using ICP-MS analysis with a 4-acid digestion at Acme Analytical Laboratories Ltd. in Vancouver, Canada. Chemical analysis of SiO_2 and FeO was performed according to standard methods described by (Jeffery and Hutchison, 1981). Further analytical details of whole rock chemical analyses are provided by (Al.Sheraefy, 2009).

PETROGRAPHY

The polished slabs (e.g. R3A and R3B, Fig. 2D) and microscopic investigations of rock-forming minerals and their textural relationships suggest that the granitoid-gabbro association in Wadi Rashid is generally marked by an abrupt change in grain size and mineralogy as response to the gabbroic magma being intruded against cold granitoid rocks. The slightly deformed granitoid (Fig. 2A) occasionally remains in a solid form or is partially split into plagioclase-rich

porphyroclasts and thermally mobilized granitoid anatectic melt ; the latter mainly comprises a polygonal texture of Na-rich alkali feldspar (e.g. anorthoclase, Fig. 3B).

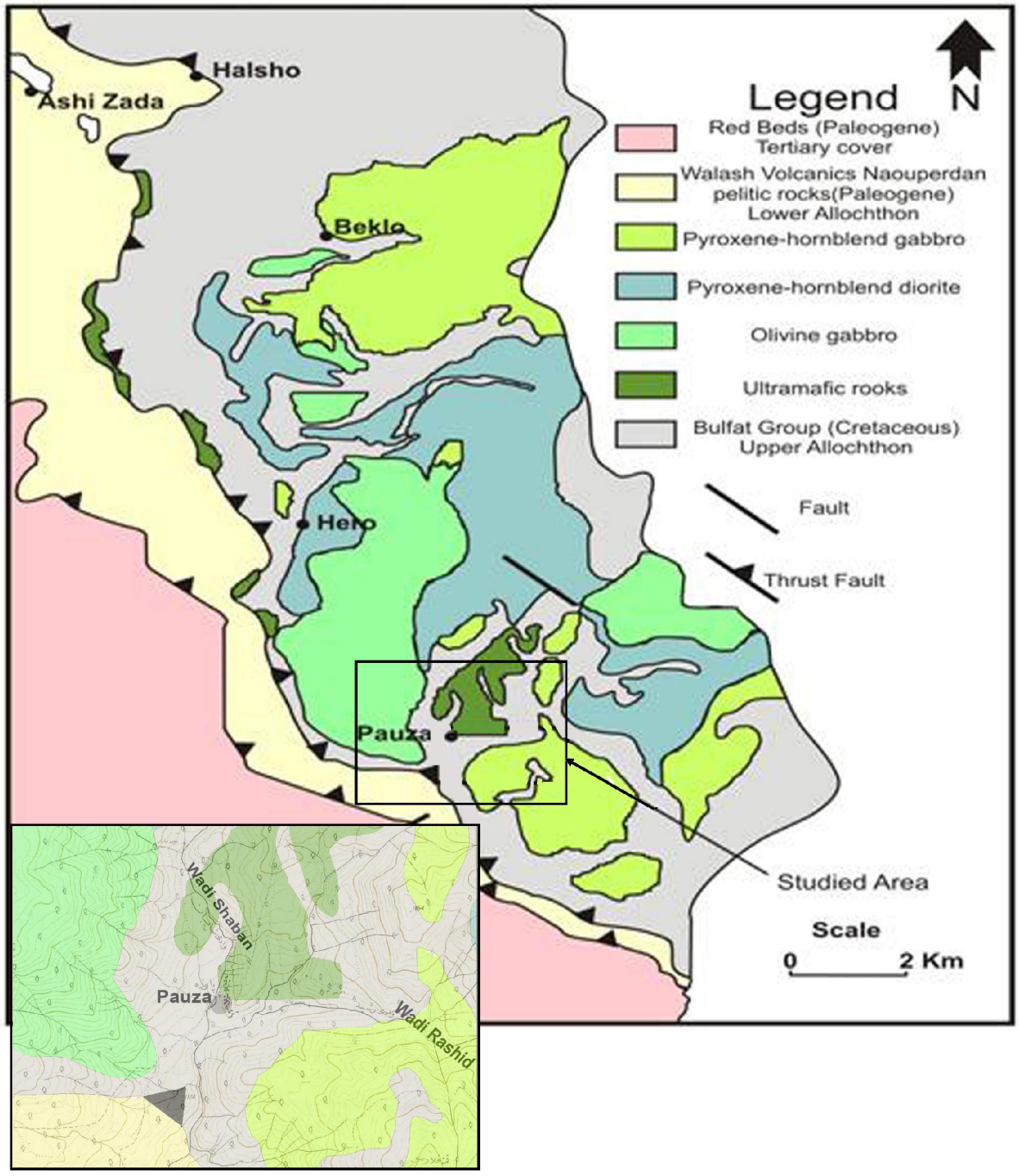

Fig. 1: Geological Map of Bulfat Complex, Qala Deza, NE IRAQ (after Geosurv-Iraq, 2002; Modified by AlSheraefy, 2009).The inset Illustrates the Geological Map Around Pauza.. Wadi Rashid ,The Dissected Valley Cuts through Pyroxene-Hornblende Gabbros.

The mixing-mingling between granitoid and gabbroic magma caused resorption of liquidus plagioclase and the formation of new Na-rich alkali feldspar crystals due to equilibration with the anatectic melt. The pre-mixed plagioclase crystals are occasionally mantled by polygonal alkali feldspar forming texture mimic anti-rapakivi texture (Fig. 3E). The narrowing of the micro-scale mineralogical gap reflects a significant assimilation of granitoid anatectic melt by the intruding gabbroic magma and clearly reveals the hybrid signature of latter (Fig. 2D). The current in-situ investigation suggests that the granitoid-gabbro association has a peculiar petrological signature and provides an ultimate indication of the occurrence of open-system processes for multiple-sources (e.g., assimilation of granitoid anatectic melt and fractional crystallization of the intrusive gabbroic magma).

In thin section, clinopyroxene grains occur as partly resorbed euhedral to subhedral crystals but never occur as interstitial grains (Fig. 3C). In melanocratic rocks, for instance, there are numerous intergrowths of pyroxene and amphibole indicating that clinopyroxene grains are partly replaced by orthomagmatic brown hornblende during magmatic evolution (Fig. 3C). The resorbed relicts of clinopyroxene in the composite 'ganitoid-gabbro suite' preserves its primary igneous characteristics during agpaitic processes (i.e. brown hornblende and aenigmatite occasionally replaced the clinopyroxene and Fe–Ti oxides, (Fig. 3D) in the leucosome unit as well as in the melanosome unit. The melanosome–leucosome contact is generally marked by an abrupt change in grain size and mineralogy, with a strong tendency for pyroxene and brown hornblende crystals to form clusters (Fig. 3D). The clinopyroxenes in the leucocratic granitoids are often observed as colorless relicts (i.e. xenocryts). Fe–Ti oxides are replace by small crystals of aenigmatite (Na–Fe–Ti silicate; Fig. 3D).The latter is usually found exhibiting a brown or black colour. In general, the ilmenite and rim of Ti-Fe-silicate (i.e. aenigmatite or Ti-rich Fe-biotite) are themselves enclosed in amphibole. It is concluded that the petrographic investigation of the melanocratic 'gabbroic' matrix reveals that there is a shift towards agpaitic mineral constituents (Fig. 3D).

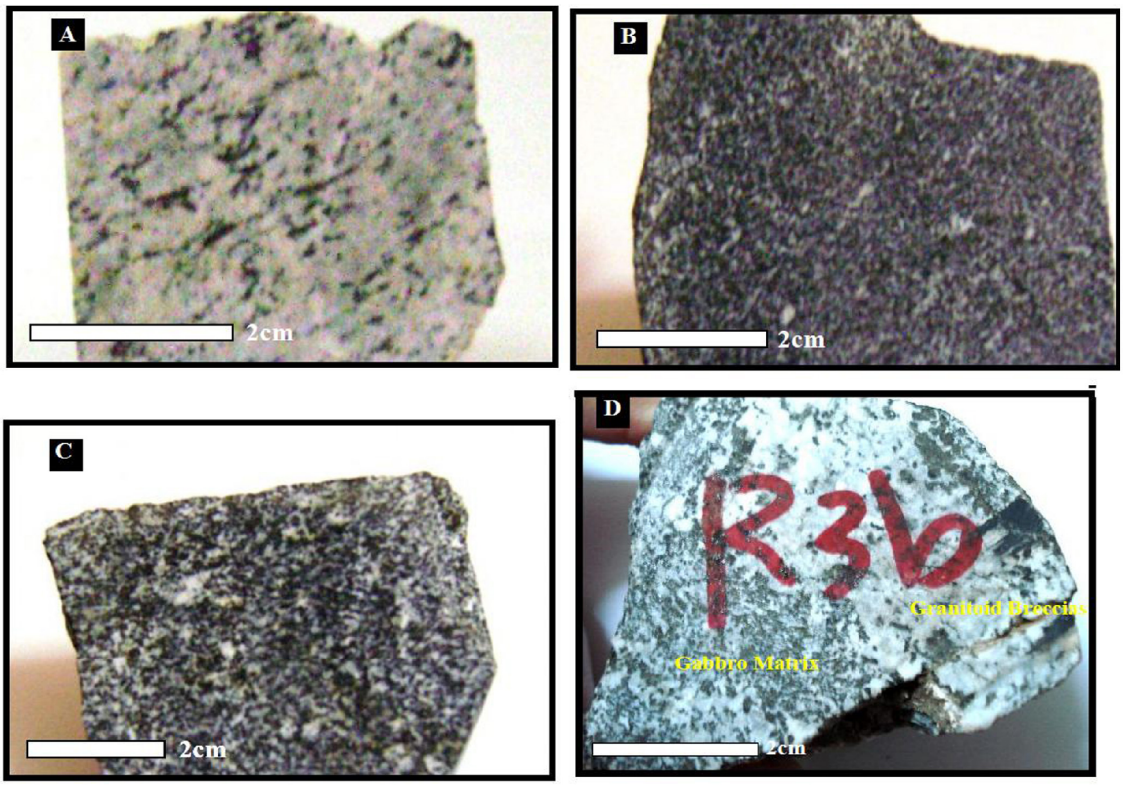

Fig . 2: Photographs of representative samples of the composite rocks 'ganitoid-gabbro suite ' from Wadi Rashid. A) Pseudogranioid gneiss' ductile deformed leucosome' with foliation of pyroxene (R6). (B) Melanosome shows rhythmic Layering of R13 showing labradorite (light) and mafic minerals (i.e. augite and hornblende (dark) (see Fig. 3F and 3G for more information). C) Melanocratic 'gabbroic' rock sample showing a dark irregular crystal of magmatic kaersutite (R4). D) The polished slabs of granitoid-gabbro association is generally marked by an abrupt change in grain size and mineralogy as response of gabbroic magma intruded against cold granitoids (R3A and R3B).

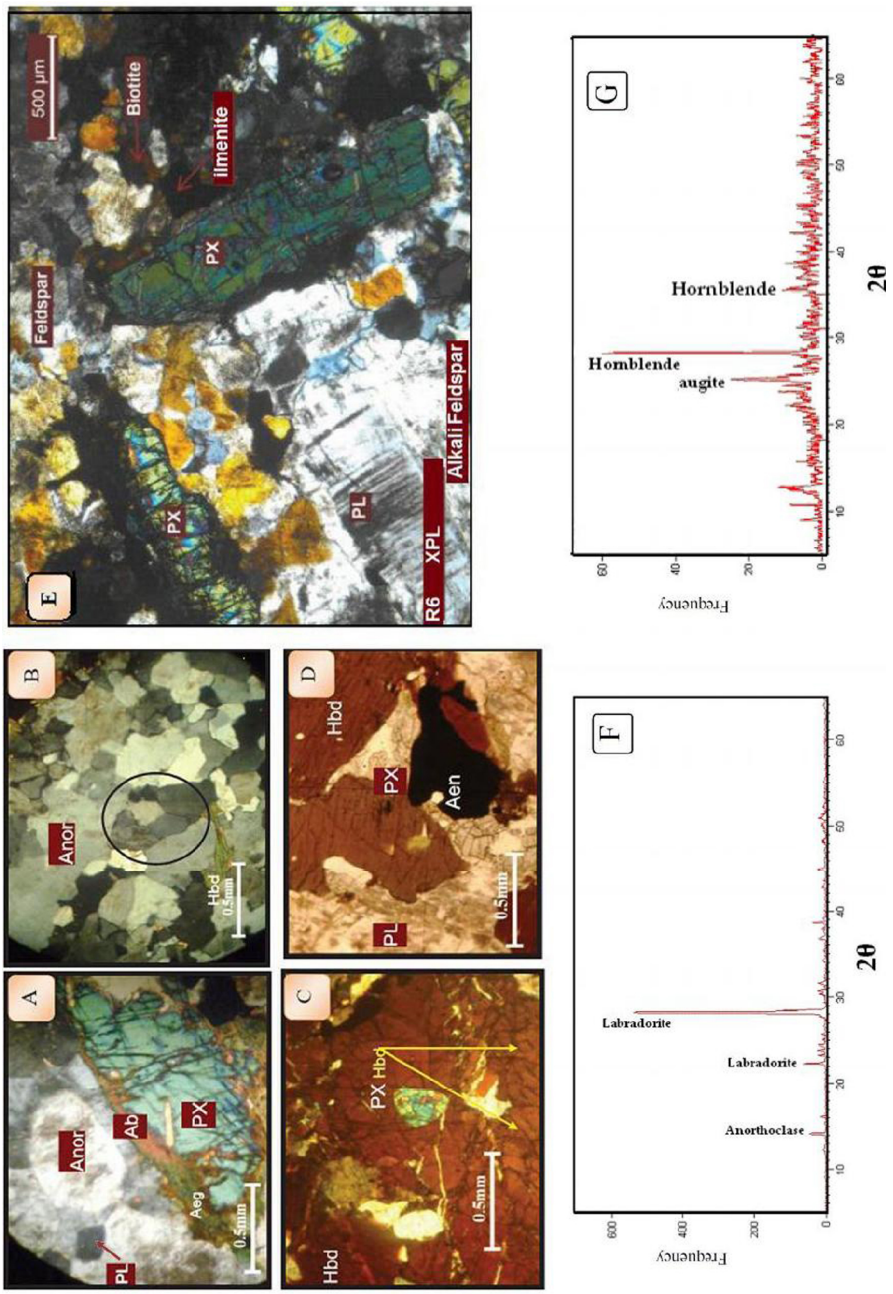

Fig. 3: Photomicrographs of selected samples used for mineral microprobe analysis (polarized light). (A-D). **A**: Photomicrograph of R6 shows resorption of liquidus plagioclase (PL) and the formation of new Na-rich alkali feldspar crystals (Ab, albite; Anor, anorthoclase) due equilibration with the anatectic melt and augite relics (PX) completely surrounded by a narrow rim of aegirin. **B**: Photomicrograph of R3B illustrating anatectic melt encompass the prevalence crystals of homogeneous-polygonal anorthoclase showing triple -point junction. **C**: Photomicrograph of R13 showing augite relic (PX) surrounded by hornblende 'kaersutite ' (Hbd). **D**: Crystal of aenigmatite (black) partly enclosed by augite(PX) and hornblende 'kaersutite ' (Hbd). **E**: Photomicrograph of R6 illustrating crystals of ilmenite (black) partly surrounded by a Ti rich Fe-Biotite as well as anti-rapakivi texture (e.g. plagioclase (PL) crystals ringed with alkali Feldspar). **F**: XRD patterns of non-magnetic fraction of R13 indicates that the dominant felsic minerals are labradorite with negligible amount of anorthoclase. G:XRD patterns of less magnetic fraction (at 60-1.0 AMPS) of the sample R13 showsthat the dominant mafic minerals are hornblende followed by augite (Photographs of the sample shown in Fig. 2B).

MINERAL CHEMISTRY AND P-T CONDITIONS

The bulk composition of the granitoid-contaminated gabbroic magma, coupled with magmatic conditions (i.e. temperature, oxygen fugacity (fO_2) and water fugacity (fH_2O)) have greatly influenced mineral compositions. Therefore, the mineral assemblages and their compositions can be used to determine the likely magmatic conditions during their crystallization. Chemical analyses for most widespread minerals of the studied rocks from Wadi Rashid area are shown in Table 1.

Plagioclase

Microprobe analyses of plagioclase in the leucosome (R6 and R8) and melanosome (R2 and R4) samples are provided in Table 1. The anorthitic component (An) of normally zoned plagioclase crystals ranges between oligoclase (An_{15} to An_{12}) and andesine (An_{22} to An_{18}) for the leucosome and melanosome, respectively, whereas anorthoclase is quite homogeneous in composition. There are noticeable differences between the compositions of plagioclase crystals in the various rock groups ranging from labradorite (Fig. 3F) to oligoclase.

Table 1: Microprobe Analyses of Feldspar from Wadi Rashid Granitoid-Gabbro Suite.

	Feldspar								
Sample Number	R6- 1	R6- 2	R8- c1	R8 - r1	R2- c1	R2 - r1	R4 - 1	R4 -2	R4 - c1
SiO_2	65.041	65.495	64.041	64.485	63.098	63.705	62.418	62.688	62.330
TiO_2	0.027	0.020	0.011	0.018	0.018	0.032	0.042	0.031	0.042
Al_2O_3	21.235	21.609	21.977	21.953	22.424	22.388	23.385	23.150	23.020
Cr_2O_3	0.000	0.012	0.031	0.043	0.000	0.000	0.000	0.000	0.019
FeO^t	0.081	0.084	0.064	0.239	0.079	0.129	0.090	0.055	0.053
MnO	0.004	0.000	0.000	0.017	0.011	0.000	0.012	0.004	0.003
MgO	0.002	0.000	0.000	0.013	0.017	0.011	0.000	0.000	0.026
CaO	2.611	2.786	3.364	3.197	4.057	4.013	4.792	4.533	4.826
Na_2O	10.813	10.714	10.075	10.254	9.705	9.778	9.318	9.464	9.269
K_2O	0.177	0.144	0.242	0.347	0.559	0.380	0.467	0.391	0.452
Total	99.991	100.865	99.805	100.564	99.968	100.437	100.524	100.314	100.039
Number of Ions calculated on 8 oxygen basis									
Si	2.849	2.848	2.822	2.819	2.779	2.795	2.740	2.756	2.750
Ti	0.001	0.001	0.000	0.001	0.001	0.001	0.001	0.001	0.001
Al	1.096	1.107	1.141	1.131	1.164	1.157	1.210	1.199	1.197
Cr	0.000	0.000	0.001	0.001	0.000	0.000	0.000	0.000	0.001
Fe^{2+}	0.003	0.003	0.002	0.009	0.003	0.005	0.003	0.002	0.002
Mn	0.000	0.000	0.000	0.001	0.000	0.000	0.000	0.000	0.000
Mg	0.000	0.000	0.000	0.001	0.001	0.001	0.000	0.000	0.002
Ca	0.123	0.130	0.159	0.150	0.191	0.189	0.225	0.213	0.228
Ba	0.000	0.000	0.000	0.000	0.000	0.000	0.000	0.000	0.000
Na	0.918	0.903	0.861	0.869	0.829	0.832	0.793	0.807	0.793
K	0.010	0.008	0.014	0.019	0.031	0.021	0.026	0.022	0.025
Molecular Ratio									
An	11.663	12.470	15.370	14.422	18.204	18.111	21.575	20.488	21.800
Ab	87.398	86.766	83.314	83.713	78.807	79.849	75.924	77.410	75.767
Or	0.939	0.765	1.316	1.866	2.989	2.039	2.501	2.103	2.433

Clinopyroxene

Since the intrusive rocks at Wadi Rashid comprise a variety of petrographically diverse rocks of contrasting composition (i.e. gabbroic and granitoid), they are well suited for a study of the influence of granitoid assimilation processes on the composition of clinopyroxene. This assumption is primarily based on the facts that: 1) clinopyroxene is often the sole liquidus phase to be preserved during the assimilation process (Nisbet and Pearce, 1977) and 2) it is an ubiquitous mineral in the studied rocks. The studied clinopyroxene in the 'ganitoid-gabbro suite ' at Wadi Rashid has preserves its primary igneous characteristics during agpaitic processes in the leucosome (i.e. R1, R3B, R6, R6A, R7A and R 8) as well as in the melanosome (i.e. R2, R4, R3A, R9, R11 and R 13)(i.e. restricted chemical composition of primary clinopyroxene).

The compositions of pyroxenes are represented in the wollastonite-enstatite-ferrosilite triangular plot (Fig. 4A). The majority of clinopyroxenes (Table 2, R6-r1, R6-c1 and R6-c2 from leucocratic 'granitoid' rocks and R8-c1 and R2-c1 from melanocratic ‘gabbro’) exhibit limited compositional variation within the diopside field (i.e. Wo_{46-49}-$En_{36-35}Fs_{18-16}$). According to the J-Q diagram, which is based on the nomenclature fields of Morimoto etal.(1988; Fig. 4A), the pyroxene grains from Wadi Rashid belong to the Ca-Mg-Fe pyroxene 'quadrilateral' field (i.e. J/(Q + J)> 0.2 and Q+J> 1.5) (Fig. 4A).

Clinopyroxenes from the ganitoid-gabbro suite are distinguished mainly by high SiO_2 (49.95-52.04 wt.%), MgO (11.18-11.58 wt.%), Na_2O <1.149 (<9 mol. % aegirine Ae) K_2O <0.013, Al_2O_3 <2.002, TiO_2 <0.56 and Cr (typically, below detection). Generally, the gabbro in the studied area does not represent a parental magma because the Cr_2O_3 values of pyroxenes are below detection limit, suggesting differentiation of the parental magma before gabbro formation. Silica undersaturation favours tetrahedral Si substitution by Al whereas increasing pressure causes preferred Al substitution in the octahedral site and results in an increased Al^{VI}/Al^{IV} ratio. The Al^{VI}/Al^{IV} ratio seems to be related to crystallization pressure for clinopyroxene (Thompson, 1974; Wass, 1979). However, the crystallization pressure for Wadi Rashid clinopyroxenes (Al^{VI}/Al^{IV} = 0.27-0.68) is low and they plot within the “igneous clinopyroxene” field on the Al^{IV} vs. Al^{VI} diagram from Aoki and Shiba (1973) as shown in Figure 4B. Based on the fact that the solubility of Ti in pyroxene increases with increasing temperature whereas it decreases with increasing pressure (Yagi and Onuma 1967, Sepp and Kanzmann 2001), the crystallization temperature of Wadi Rashid clinopyroxenes (Ti = 0.011-0.14 apfu) is below 900°C (Fig. 4C). Crystallization pressures for clinopyroxenes were determined using a formulated empirical geobarometer proposed by Nimis (1995) on the basis of the unit-cell volume (V_{cell}) vs. M1-site volume (V_{M1}) relationship. The calculations of crystallization pressure using the V_{cell}–V_{M1} relationship for Wadi Rashid range from 60 to 260 MPa (i.e. 1 kbar= 100 MPa).

Table 2: Miroprobe Pyroxene Analyses of Pyroxene from Wadi Rashid Granitoid-Gabbro Ssuite.

Rock Type	**Pyroxene**					
Sample Number	R6-r1	R6-c1	R6-c2	R8-c1	R2-c1	R4-c
SiO_2	51.705	51.979	51.617	52.043	50.542	49.945
TiO_2	0.46	0.404	0.461	0.48	0.507	0.556
Al_2O_3	1.316	1.391	1.255	1.551	2.002	1.896
fe_2O_3	0	0	0	0	0	0
Cr_2O_3	0	0	0	0	0.036	0
FeO	13.145	13.03	13.091	11.978	13.133	13.457
MnO	0.471	0.515	0.436	0.376	0.405	0.431
MgO	11.32	11.274	11.178	11.289	11.581	11.387
CaO	21.305	21.218	21.558	21.728	20.585	20.046
Na_2O	0.883	0.915	0.899	1.149	0.807	0.714
K_2O	0	0	0	0	0.015	0.013
Total	100.605	100.727	100.494	100.594	99.611	98.445
Si	1.944	1.951	1.943	1.947	1.916	1.920
Ti	0.013	0.011	0.013	0.014	0.014	0.016
Al^{IV}	0.043	0.038	0.044	0.039	0.070	0.064
T site	2.000	2.000	2.000	2.000	2.000	2.000
Al^{VI}	0.015	0.024	0.012	0.029	0.019	0.022
Fe^{+3}	0.093	0.080	0.098	0.093	0.110	0.097
Fe^{+2}	0.320	0.329	0.314	0.281	0.307	0.336
Mn	0.015	0.016	0.014	0.012	0.013	0.014
Mg	0.557	0.551	0.562	0.584	0.550	0.532
M1 site	1.000	1.000	1.000	1.000	1.000	1.000
Mg	0.078	0.080	0.065	0.046	0.104	0.121
Ca	0.858	0.853	0.869	0.871	0.836	0.826
Na	0.064	0.067	0.066	0.083	0.059	0.053
K	0.000	0.000	0.000	0.000	0.001	0.001
M2 site	1.000	1.000	1.000	1.000	1.000	1.000
Wo	47.33	47.07	48.01	48.88	46.52	45.51
En	34.99	34.8	34.64	35.34	36.41	35.97
Fs	17.68	18.13	17.35	15.79	17.07	18.52
Total	100	100	100	100	100	100
Q	1.73	1.73	1.75	1.74	1.69	1.69
J	0.13	0.13	0.13	0.17	0.12	0.11

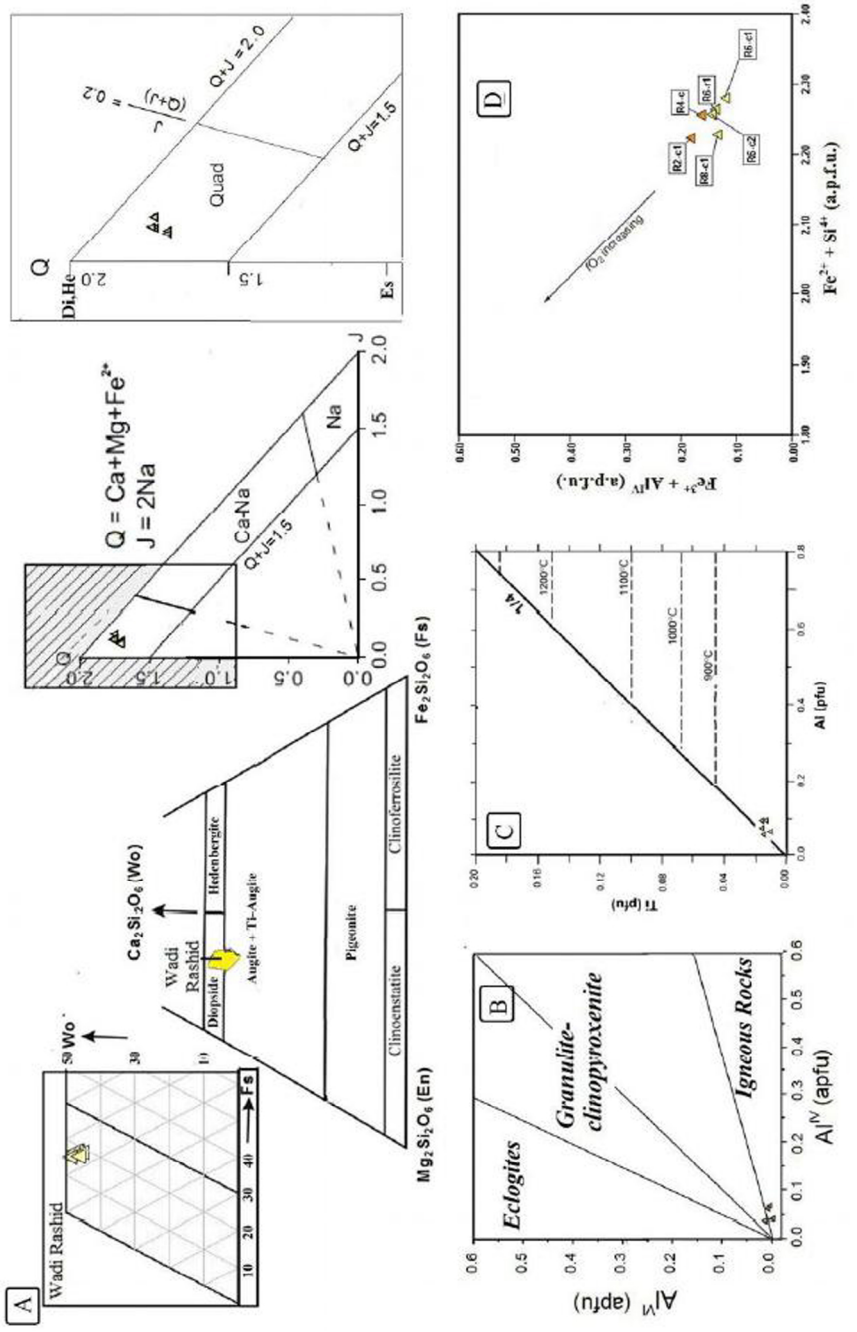

Fig. 4 : **A**: Plot of clinopyroxene compositions of Wadi Rashid in the En—Wo—Fs ($Mg_2Si_2O_6$—$Ca_2Si_2O_6$—$Fe_2Si_2O_6$) diagram with the nomenclature fields of Morimoto *et al.*, (1988). **B** : Al^{IV} vs. Al^{VI} diagram of Aoki and Shiba (1973) shows that the crystallization pressure of WR clinopyroxenes is low and they plot within "igneous clinopyroxene" field. **C:** A plot of Ti vs Al concentrations (Yagi and Onuma 1967, Sepp and Kanzmann 2001), illustrate that the crystallization temperature of WR clinopyroxenes is slightly below 900 ^{o}C, **D:** Fe^{2+}+Si^{4+}–Fe^{3+}+Al^{IV} relationships for WR clinopyroxenes, showing the negligible increasing fO_2 during the during agpaitic processe. Data from Table 1; a.p.f.u. = atoms per formula unit.

Ti-rich Silicates

Amphibole

Primary amphibole is the most abundant mafic mineral in the studied rocks. It is essentially homogeneous in composition, and corresponds to K–Ti-enriched (ca. 0.20 *apfu* K, 0.50 *apfu* Ti) hornblende (Table 3, anal. 3 - 4) and lies in the field of Ti-rich pargasite (kaersutite; Leake *et al.,* 1997). It is evident from mineral composition that kaersutite in the melanosome (i.e. R4) crystallized at a high temperature deduced from its high Ti, Al^{IV} $(Na+K)^{A}$ values (Raase, 1974; Ernst and Liu, 1998), (Bard, 1970; Blundy and Holland, 1990) and. Based on the empirical thermo-barometric formulations of Ridolfi *et al.*, (2010), the *P*-*T*, logfO_2-*T*, and *T*-H_2O show that the primary 'orthomagmatic' kaersutite equilibrated at a nearly constant pressure of about 269-277 MPa and at temperatures of crystallization of about 933–935°C. The logfO_2 during equilibration of kaersutite in the hosting melanosome (i.e. R4) is in the range of -12.2 to -12.4 (Δlog fO_2 (NNO) ~ -1) and melt water contents slightly higher than 4 wt.%. The relatively high oxidation state (i.e. $Fe^{3+}/\Sigma Fe$ ratio = 0.034 - 0.087) in the amphiboles from the melanosome (i.e. R4) reveals the presence of an oxy-component in the kaersutitic amphiboles composition. Application of the hornblende–plagioclase thermometer (Blundy and Holland, 1990) on the amphiboles in the leucosome (R8) and contaminated melanosome (R2) indicates a relatively low temperature (~753°C) in comparison with that of the melanosome at presumably the same presuure stated above. These minor compositional differences, in particular the $Fe^{3+}/\Sigma Fe$ ratio content between the amphiboles in the melanosome (R4) and leucosome (R8) are possibly related to reducing conditions during crystallization and a late-stage granitoid assimilation overprint on the contaminated gabbroic magma.

Biotite

Textural and petrological studies indicate that the biotite in R6 is a subsolidus phase, partly replacing the nearly pure ilmenite (+ anorthoclase) (Fig. 3E). The composition of the biotite is Fe- and Ti-rich and Al-poor, taken in conjunction with (Fe exclusively present as Fe^{2+}). Accordingly, the biotite is classified as Fe-biotite on the Foster classification diagram (Foster, 1960). Ti is preferentially partition into biotite as a function of temperature (Henry and Guidotti, 2002), and the Fe/Mg ratio decreases with increasing temperature (Ferry and Spear, 1978). The studied Fe-biotite has a Ti content = 0.33, and a Fe/Mg ratio = 3.2. The estimation temperature of Fe-biotite in R6 is 647°C, using the empirical Ti-in-biotite geothermometer of Henry and (Guidotti, 2002).

Based on the experimentally calibrated curve of Wones and Eugster (1965), the oxygen fugacity of the studied Fe-biotite is below QMF.However, the ilmenite replacement process is the result of an appreciable amount of H_2O (several wt. % of H_2O) that is required to stabilize Ti-rich Fe-biotite. A notably absent phase in R6 (leucosome) is hornblende (Fig. 3E). It is presumably that the latter is not stable at H_2O saturated condition with temperature about (i.e. =647°C).

Table 3: Microprobe Analyses of Amphibole and Biotite from Wadi Rashid Granitoid- Gabbro Suite.

Rock Type	Amphibole						
Sample Number	R4-1	R4-2	R4A-3	R8-c1	R8-c2	R2-1	R2-2
SiO_2	41.38	41.96	41.67	41.60	41.56	41.43	41.54
TiO_2	4.52	4.45	4.91	4.30	4.27	4.51	4.54
Al_2O_3	10.36	10.61	10.43	10.37	10.30	10.20	10.34
FeO	16.90	16.90	16.99	17.58	17.46	17.42	17.35
MnO	0.32	0.31	0.29	0.39	0.31	0.37	0.37
MgO	9.99	10.34	10.01	9.55	9.51	9.49	9.67
CaO	10.89	10.91	10.87	11.14	11.07	11.02	11.04
Na_2O	3.22	3.14	3.30	3.32	3.44	3.12	3.08
K_2O	0.74	0.79	0.73	1.06	0.91	0.97	0.99
Cr_2O_3	0.03	0.05	0.01	0.05	0.00	0.02	0.03
Total	98.3452	99.4899	99.2163	99.3614	98.842	98.5538	98.9401
Formula on the basis of 13 cations (Leake et al 1997)							
Si	6.233	6.222	6.223	6.261	6.285	6.270	6.250
Al^{IV}	1.767	1.778	1.777	1.739	1.715	1.730	1.750
Ti	0.000	0.000	0.000	0.000	0.000	0.000	0.000
Al^{VI}	0.072	0.077	0.059	0.101	0.121	0.090	0.084
Ti	0.512	0.497	0.552	0.487	0.486	0.514	0.514
Cr	0.004	0.006	0.001	0.006	0.000	0.003	0.003
Fe^{3+}	0.071	0.182	0.041	0.000	0.000	0.000	0.000
Mg	2.243	2.285	2.229	2.143	2.144	2.141	2.169
Fe^{2+}	2.057	1.915	2.081	2.213	2.208	2.205	2.183
Mn	0.041	0.039	0.037	0.050	0.040	0.048	0.047
Csite	5.000	5.000	5.000	5.000	5.000	5.000	5.000
Fe^{2+}	0.000	0.000	0.000	0.000	0.000	0.000	0.000
Ca	1.757	1.733	1.739	1.796	1.794	1.787	1.780
Na	0.243	0.267	0.261	0.204	0.206	0.213	0.220
Bsite	2.000	2.000	2.000	2.000	2.000	2.000	2.000
Na	0.697	0.637	0.694	0.765	0.804	0.701	0.679
K	0.142	0.150	0.139	0.204	0.176	0.187	0.191
Asite	0.840	0.787	0.833	0.969	0.980	0.887	0.870
$Mg/Mg+Fe^{2+}$	0.522	0.544	0.517	0.492	0.493	0.493	0.498

biotite, R6	
Oxide	Wt.%
SiO_2	34.81
TiO_2	5.38
Al_2O_3	13.57
Fe_2O_3	0
FeO	27.95
MnO	0.19
MgO	4.89
CaO	0.26
Na_2O	0.11
K_2O	9.37
Total	96.52
Oxygens per formula = 11	
Si	2.800
Al	1.200
total	4
Ti	0.325
Fe^{+3}	0
Fe^{+2}	1.880
Mn	0.0132
Mg	0.586
Total(M)	2.889
Ca	0.022
Na	0.016
Total(I)	1

Aenigmatite

Textural evidence (e.g. R7A, Fig. 3D) advocates that aenigmatite coexisted with augite and kaesutite. Ilmenite was completely substituted by aenigmatite due to the interaction of liquidus phases with thermally mobilized peralkaline 'granitoid' anatectic melt. The opposed occurrence of aenigmatite and ilmenite suggests that a reaction relationship between these liquidus phases required a melt peralkalinity index [PI = molar $(Na_2O+K_2O)/Al_2O_3$] higher than 1·2 and pressures >100 MPa. (Di Carlo et al., 2010). The antipathetic occurrence of these phases (i.e. aenigmatite and ilmenite) may be also attributed to the peritectic relationship with each other (Nicholls and Carmichael, 1969) as a result of the peralkalinity shift during agpaitic processes.

Fe-Ti oxides

Nearly pure ilmenite ($Ilm_{96–99}$) is a widespread Fe-Ti oxide in both the leucosome (e.g. R6, and R8) and melanosome (e.g. R2) and it consistently has a high MnO content ($MnTiO_3$ < 4 mole %), very low concentrations of Al_2O_3, MgO, Cr_2O_3 and Ti-excess over their ferrous end members (Table 4). The small Ti excess might be related to cationic vacancies (Lattard et al., 2005). Ilmenite within R6 has $FeTiO_3$ amounts usually above 99 mol. % and it is surrounded by a rim of Ti-rich Fe-biotite (Fig. 3E). An interesting point is that at a temperature exceeding 600°C, the isopleths for nearly pure ilmenite are practically independent of temperature with rather low oxygen fugacities (Andersen and Lindsley, 1988; Ghiorso and Sack, 1991). For sample R6, however, the negligible hematite contents in early-formed ilmenite reveal that the early development of the leucosome was at an apparently low oxygen fugacity ($\Delta\log fO_2$ (FMQ) ~ -4), with Fe dominantly present as Fe^{2+}, Except for sample R7A (Fig. 3D). Ilmenite was the earliest-formed Ti-bearing phase, but it became unstable in the peralkaline 'granitoid' anatectic melt and consequently it was apparently replaced by aenigmatite + kaesutite at a relatively higher oxygen fugacity ($\Delta\log fO_2$ (FMQ) ~1) than that of ilmenite-Fe-biotite assemblages.

Titano magnetite (i.e. magnetite–ulvöspinel solid solution) was found only within sample R4 (melanosome) and its composition is estimated at Usp_{41} (i.e. TiO_2 = 14.292 wt %). Variation in Ti concentration in titano magnetite is potentially very sensitive to small shifts in fO_2 and T and its composition is significantly richer in Ti at low fO_2 and high T (Andersen and Lindsley, 1988). In sample R4, the titano magnetite isopleth of Usp_{40} at T ~ 934°C indicates that the fO_2 is within ~1 log unit of the quartz–fayalite-magnetite buffer (i.e. $\Delta\log fO_2$ (FMQ) = ~1). This coincides with the $\log fO_2$ of kaersutite in the same studied sample (i.e. R4) which is in the range of -12.2 to - 12.4. Whereas the ilmenite hosting rocks (i.e. R2, R6, and R8) yield the lowest oxygen fugacities (e.g. $\Delta\log fO_2$ (FMQ) ~ -4).

Table 4: Microprobe Ilmenite and Titano Magnetite from Granitoid-Gabbro of Wadi Rashid.

Imenite			
Sample No.	R6	R8	R2
Oxide	Wt.%		
SiO_2	0	0	0
TiO_2	50.08	50.64	51.26
Al_2O_3	0	0	0
Cr_2O_3	0	0	0
Fe_2O_3	3.9996	3.333	0.556
FeO	43.4	42.61	43.78
MnO	1.71	2.1	1.65
MgO	0.06	0.32	0.34
CaO	0.03	0.02	0
Totals	99.27	99.043	97.61
Si	0	0	0
Ti	0.960	0.970	0.995
Al	0	0	0
Cr	0	0	0
Fe^{+3}	0.077	0.064	0.011
Fe^{+2}	0.925	0.907	0.945
Mn	0.037	0.045	0.036
Mg	0.002	0.012	0.013
Ca	0.001	0.001	0
Na	0	0.001	0.001
	2.002	1.999	2.000

Titano magnetite	
R4	
Oxide	Wt.%
SiO_2	2.41
TiO_2	14.29
Al_2O_3	1.43
Cr_2O_3	0.24
Fe_2O_3	28.96
FeO	44.26
MnO	1.18
MgO	0.09
Totals	92.86
Formula on the basis 4 Oxy.	
Si	0.096
Ti	0.430
Al	0.067
Cr	0.007593
Fe^{+3}	0.872093
Fe^{+2}	1.481076
Mn	0.039993
Mg	0.005369

WHOLE-ROCK GEOCHEMISTRY

Wadi Rashid intrusive rocks represent a bimodal granitoid-gabbro suite, with the absence of rocks of intermediate composition (especially in the range 50–60 wt.% SiO_2, the so-called Daly Gap). Mingling of the gabbro magma with coeval granitoid was hoticed in the field. Concerning bimodality, the rare earth element (REE) data (Table 5) confirm an apparent enrichment in all the REEs (total REE) in the melanocratic 'gabbroic' rocks relative to leucocratic 'granitoid' rocks in Wadi Rashid suite where the total REE contents are 216-556 ppm and 559-1055 ppm for leucocratic and melanocratic rocks, respectively. This contradicts a basic principle suggesting that with increasing differentiation, silicic rocks are marked by increases in their REE contents. Accordingly, the granitoid and gabbro of Wadi Rashid have their own geochemical characteristics indicating different sources.

It is evident from our in-situ field inspection of the mingling phenomena that the Daly Gap is a function of density contrast (Weaver, 1977) between leucocratic 'granitoid' breccias and melanocratic 'gabboic' matrix. The Daly Gap may be

attributed to the variations in magma residence time and cooling rate that can lead to large thermal and compositional swings, interrupting the assimilation process and causing bimodality in the rock suite (Bonnefoi *et al.,* 1995). The detailed microscopic investigations of mineral constituents and their textural relationships (e.g. grain size and mafic mineral distributions) suggest that the thermal budget of the gabbroic magma played a major role in the bimodality between gabbroic melt and the coeval granitoid melt. It is evident from the in-situ field inspection that the spectrum of composite intrusive rocks clearly grade into each other, therefore the terms gabbro and granitoid are simply used to provide a working nomenclature for the individual rock types. In view of this aspect the geochemistry of each rock-type (i.e. granitoid and gabbro) and their tectogenesis are discussed separately.

Table 5: Major oxides and trace element analyses from Granitoid - gabbro of Wadi Rashid, as determind ICP-MS(ACME Laboratories).

Samples	**Leucocratic**						**Melanocratic**					
Major Oxides (wt %)	R1	R3B	R6	R6A	R7A	R8	R2	R3A	R4	R9	R11	R13
SiO_2	61.08	60.52	62.88	60.92	61.97	60.66	49.78	47.25	48.99	48.99	50.98	48.52
TiO_2	0.75	1.29	1.08	1.15	0.93	1.15	2.84	2.79	2.3	2.55	1.83	2.41
Al_2O_3	18.82	17.57	16.74	17.23	18.08	17.65	15.51	15.68	15.95	17.06	16.84	14.36
Fe_2O_3	2.3	1.64	1.05	1.96	1.68	1.35	7.08	7.76	6.59	6.18	4.61	8.21
FeO	2.61	3.54	3.36	3.37	2.79	3.75	4.88	4.59	4.73	4.63	4.59	4.16
MnO	0.09	0.09	0.07	0.09	0.07	0.1	0.24	0.23	0.22	0.19	0.18	0.21
MgO	1.19	1.96	0.76	1.08	0.8	2.06	5.26	5.29	5.77	3.83	5.44	7.1
CaO	3.81	4.74	2.87	3.43	2.74	5.28	8.45	8.84	8.45	7.54	7.93	9.45
Na_2O	7.68	7.68	8.35	8.27	8.84	7.51	5.27	5.24	5.19	6	5.65	3.98
K_2O	0.36	1.21	1.02	0.86	0.94	0.81	0.86	0.74	0.63	0.76	0.65	0.35
P_2O_5	0.22	0.35	0.26	0.32	0.11	0.32	0.62	0.7	0.48	0.47	0.34	0.26
LOI	2.32	1.15	1.2	1.31	1.02	1.21	1.01	1.73	1.38	0.82	1.62	1.25
Total	101.21	101.73	99.65	99.99	99.97	101.82	101.78	100.83	100.67	99.02	100.65	100.25
FeOt	4.68	5.02	4.31	5.15	4.31	4.97	11.28	11.6	10.69	10.21	8.76	11.58
Mg#	26.28	30.03	14.98	19.88	18.11	29.88	45.55	.	48.6	39.09	44.57	54.8
	R1	R3B	R6	R6A	R7A	R8	R2	R3A	R4	R9	R11	R13
Trace Elements (ppm)												
Sc	1.2	11.4	4.1	3.3	3.1	12.1	33.2	31.5	31.5	20.7	30.5	38.6
Cr	6	11	2	1	2	22	63	26	69	26	79	167
Ni	3.7	13.4	4.7	3.1	3.9	14.9	32.3	24.4	45.9	22	36.3	72.8
Y	7.4	35.7	17.5	25.4	8.8	36.8	76.6	70.8	60	57.8	43.9	49.4
Zr	17.7	115.1	13.5	50.8	14.1	130.9	270.7	264	202.9	215.6	216.6	32
Hf	0.35	2.95	0.39	1.29	0.38	3.33	7.46	7.06	5.46	5.7	5.04	1.61
Ta	0.9	0.7	1	0.8	0.6	0.9	1.2	1.1	1	1.4	0.9	0.7
Th	.	0.5	0.1	0.3	0.1	0.2	0.4	0.3	0.2	0.2	0.2	0.8
Mo	0.49	0.32	0.52	0.48	0.39	0.29	0.45	0.46	0.34	0.74	0.4	0.91
Cu	11.01	22.03	3.84	8.46	2.44	22.38	43.39	45.81	48.54	41.32	51.87	48.03
Pb	0.72	5.54	3.36	3.33	3.68	2.8	2.12	2.23	2.7	2.39	2.06	2.75

Samples	Leucocratic						Melanocratic					
Major Oxides (wt %)	R1	R3B	R6	R6A	R7A	R8	R2	R3A	R4	R9	R11	R13
Zn	36.5	52.3	43.7	57.9	64.6	46.1	111	102.8	103.6	96.5	79	79.9
Sr	527	329	201	213	248	333	243	292	225	284	306	207
Cd	0.04	0.16	0.05	0.12	0.09	0.17	0.36	0.39	0.37	0.28	0.29	0.13
Co	32	27.9	27.5	23.1	28.4	31.6	47.1	45.8	46.6	54.2	46.8	56.6
Ba	87	218	412	326	423	189	153	131	119	138	68	36
Sn	0.3	1.1	0.3	0.4	0.3	0.7	0.8	0.8	0.9	0.9	1.1	2.2
	R1	R3B	R6	R6A	R7A	R8	R2	R3A	R4	R9	R11	R13
Rb	7.6	9.2	5.9	4.6	5.7	4.4	5.4	5.1	2.8	4.9	5.6	4.9
Ga	12.58	18.61	15.89	17.1	15.88	18	18.74	18.91	18.95	18.61	16.66	18.24
V	42	124	34	27	31	97	278	270	255	254	217	314
Nb	1.6	10.7	3.82	9.64	2.09	11.76	24.34	21.57	15.06	19.95	10.05	7.9
Rare Erath Elements (ppm)												
La	5.6	20.6	13.2	17.9	8.2	19.9	34.4	30.1	24.3	24.2	15.6	11.1
Ce	11.18	43.19	26.59	36.96	13.95	40.64	79.15	67.43	56.4	56.29	34.84	26.41
Pr	1.6	6.1	3.7	5.2	1.9	6	11.3	10.1	8.1	8.3	5.4	4.5
Nd	6.7	26	16.2	22.9	7.8	24.6	51	45.2	37.8	36.7	24.9	22.5
Sm	1.3	5.1	3.3	4.6	1.5	5.1	10.5	10	8.1	7.6	5.4	5.8
Eu	1.5	1.7	1.8	2.2	1.7	1.7	2.6	2.7	2.3	2.3	1.8	2.2
Gd	1.5	6	3.4	4.7	1.5	5.7	12.9	10.9	8.9	10	6.7	7.7
Tb	0.2	1	0.6	0.7	0.3	1	2	1.9	1.7	1.6	1.1	1.3
Dy	1.2	6.1	3.2	4.6	1.6	6.4	13.6	11.8	10.3	10	7.3	7.9
Ho	0.3	1.3	0.6	0.9	0.3	1.3	3	2.5	2.3	2.2	1.6	1.9
Er	0.7	3.6	1.6	2.3	0.8	3.6	7.9	7.4	6.6	6.1	4.5	5
Tm	.	0.5	0.2	0.3	0.1	0.5	1.2	1	0.9	0.8	0.7	0.7
Yb	0.6	3	1.1	1.9	0.7	3.2	6.7	6.3	5.8	5.4	4.3	4.5
Lu	.	0.4	0.2	0.3	0.1	0.5	1.1	1	0.9	0.8	0.6	0.7

GRANITOID ROCKS

1- Chemical classification and petrogenesis

Wadi Rashid granitoid is geochemically classified using total alkalis versus silica (TAS) diagram (Wilson, 1989). Notably, they roughly correspond to syeno-diorite/syenite (cf. Fig. 5B), having an agpaitic index (A.I. = mol Na+K/Al) slightly less than unity (alkali metaluminous; Fig. 5C, D). But the presence of agpaitic assemblages, such as kaesutite and/or aenigmatite, may indicate that the melt composition of these rocks experienced at the microscopic scale a considerable shift from metaluminous to alkali metaluminous mineral assemblages. Based on their normative orthoclase-albite-anorthite (Or–Ab–An) contents using the classification scheme of Barker (1979), Wadi Rashid granitoid rocks cluster close to the Ab corner in the trondhjemite field (Fig. 5E). According to Barker's classification scheme, the mafic phase in the trondhjemites is usually biotite and in

most cases these rocks are REE-depleted. Thus the rocks in the present study are significantly different from typical 'trondhjemites' as defined by Barker (1979). The petrography and mineral chemistry of these rocks indicates that there are two contrasting alkali metaluminous facies: (i) Fe-biotite granitoid and (ii) kaersutite-aenigmatite granitoid. In addition, the granitoid rocks occasionally encompass primary phases of mafic origin as resorbed xenocrysts (i.e. augite, An-rich plagioclase and ilmenite). At least some of the xenocrysts were probably derived from remobilisation of partially solidified gabbroic material and mixed with anatectic granitoid melt.

Wadi Rashid granitoid rocks span a narrow range of 60-63 % SiO_2 (Fig. 5A). All are low in K_2O (<1.2%, Fig. 5F); these low-K granitoid rocks are similar to oceanic plagiogranites, which range in composition from trondhjemite to tonalite and diorite (Coleman and Peterman, 1975; Coleman and Donato, 1979). Also quite similar low-K trends are seen in primitive island arcs in the western Pacific, e.g., Izu-Bonin. However, the name 'plagiogranite' is not considered for studied granitoid rocks since plagiogranites are associated with oceanic crust plutonic suites, e.g., with ophiolite sequences (Gerlach *et al.,* 1981; Ashley *et al.,* 1983; Kontinen, 1987; Barbieri *et al.,* 1994; Borsi *et al.,* 1996; Koepke *et al.,* 2004), which is not the case for Wadi Rashid granitoid rocks. Dehydration melting experiments on natural metabasalt samples show that low-K_2O granitoid melts form in response to melting of protoliths that are initially low in K_2O to begin with, such as oceanic greenstones (Beard and Lofgren, 1991; Rapp *et al.,* 1991; Rushmer, 1991). These experiments show that a protolith with ~0.3% K_2O is needed to form melts with the low-K_2O concentrations (<1.2%) observed here.

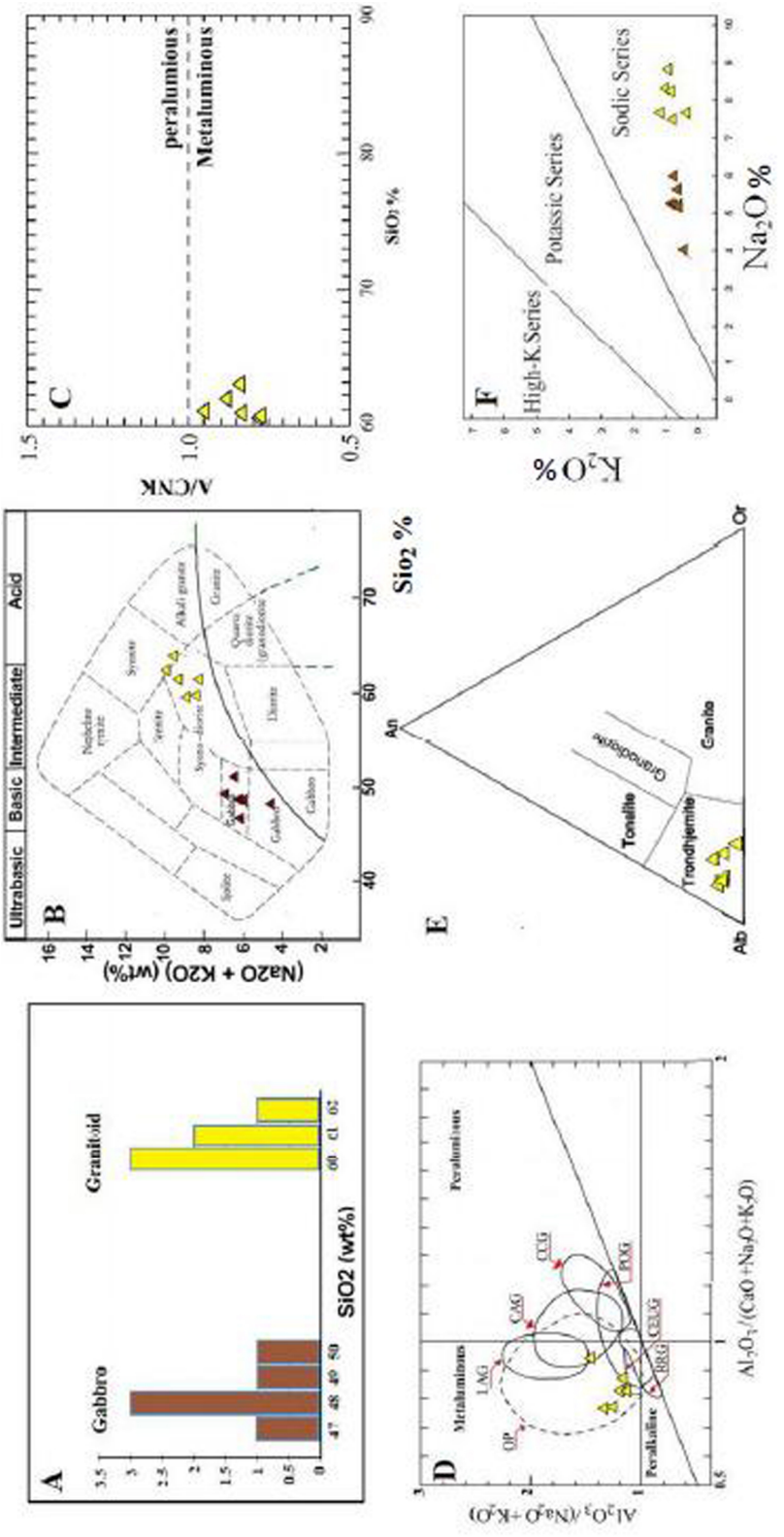

Fig. 5 **A**: SiO_2 histogram showing bimodal granitoid–gabbro suit of of Wadi Rashid intrusion. **B:** Plot of total alkalis vs silica (TAS) (Wilson, 1989) showing the compositions of Wadi Rashid. **C:** A/KNC= Al_2O_3/ (K20 +Na2O +CaO) molar vs SiO2 (Frost *et al.*, 2001). **D:** Agpaitic index, A.I= = (Na_2O+ K_2O)/Al_2O_3 vs Aluminium Saturation Index, ASI = Al_2O_3 /(CaO + Na_2O +K_2O) molar , after Maniar and Piccoli, (1989). (OP: Oceanic plagiogranite, IAG: Island Arc Granitoid, CAG: Coutinental Arc Granitoid, CCG: Continental Collision Granitoid, RRG: Rift- related granitoid. CEUG:Continental Epeirogranic Up ltift Granitoid, POG: Post Orogenic Granitoid). **E:** Tonalite-trondhjemite ternary, after Barker, (1979), based on normative anorthite-albite-orthoclase. **F:** Plot of K_2O vs Na_2O,after

2- Geochemical Signature and Tectonic Setting

REE data for Wadi Rashid granitoid rocks are given in Table 5, and chondrite normalized rare earth elements patterns are shown in Fig. 6A. This figure illustrates parallel to sub-parallel, moderately fractionated REE patterns [(La/Yb)N = 4.46-8.61, (La/Sm)N = 2.51-3.53 and (Gd/Yb)N = 4.46-8.61]. The granitoid rock samples display depleted REE- chondrite-normalized La (~87-24) and Yb (~19-4). They are enriched in the light rare earth elements (LREE) relative to the heavy rare earth elements (HREE; Fig. 6A). This enrichment is relatively modest (La/Yb ratios are 4.46-8.61× chondrite), with discernible Eu anomalies that are typically positive. Sample R7A with a low Mg# (~18%) displays a large positive Eu anomaly and lower HREE concentrations, consistent with its plagioclase abundance (Fig. 6A). The low HREE in the studied granitoid rocks seems to be due to partial melting of metamorphosed oceanic crust leaving HREE-rich accessory minerals (i.e. garnet+ hornblende) as a residual phase in the source. According to the hydration-melting experiments on metamorphosed oceanic greenstone melting depths of >48 km (i.e. 1.45GPa) are required to provide sufficient garnet in the residuum to generate the degree of heavy rare earth element depletion documented in the granitoid rock type (Nair and Chacko, 2008).

NMORB normalized trace element patterns for Wadi Rashid samples (Fig. 6B) display enrichment in large ion lithophile elements (LILE; Rb, Ba and K) and depletion in high field strength elements (HFSE; Nb, Hf, Zr and Ti). These characteristics are diagnostic of rocks formed in subduction related settings (e.g. Pearce and Parkinson, 1993). On a multi-element diagram, the samples show both negative and positive peaks for Sr and Ti, which are interpreted to be due to variation in feldspar and Ti-rich phases (ilmenite, Ti-rich magnetite, aenigmatite and Ti-rich Fe-biotite). The negative Th anomaly is well expressed whereas for many, indeed most, silicic rocks, increasing differentiation is marked by an increase in Th content (e.g. Stuckless *et al.,* 1977). The lack of enrichment of this element in Wadi Rashid granitoid rocks implies that this element was mobilized by some late- or post-magmatic process.

The conclusion drawn from REE and MORB-normalized multi-element characteristics (i.e. positive LILE and negative HFSE anomalies) is supported by granitoid trace-element discrimination diagrams based on Y, Yb, Nb, Ta and Rb (Pearce *et al.,* 1984). Pearce et al. (1984) classified granitoid rocks into four main groups: ocean-ridge granites (ORG), volcanic-arc granites (VAG), within-plate granites (WPG), and collision granites (COLG). In the trace element tectonic discrimination scheme for granites (Pearce *et al.,* 1984), Wadi Rashid granitoid rocks show volcanic-arc granite characteristics (Fig. 7).

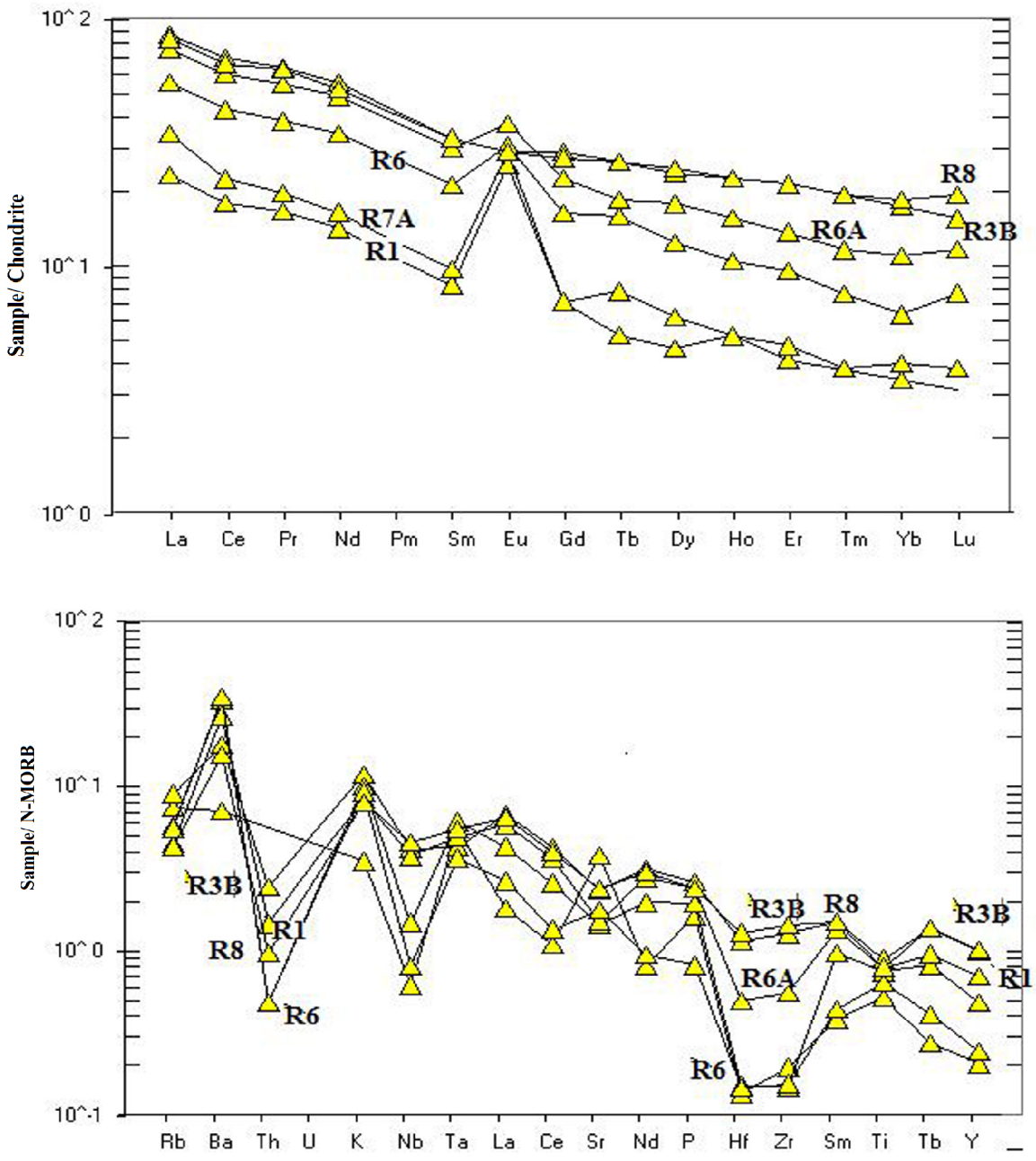

Fig. 6: Chondrite-Normalized Rare Earth Element (REE) Patterns (Upper Figure) and NMORB-Normalized Ttrace Element Patterns (Lower Figure) of the Wadi Rashid Granitoid. The Chondrite and NMORB Mantle Values are from Sun and McDonough (1989) and McDonough and Sun (1995), Respectively.

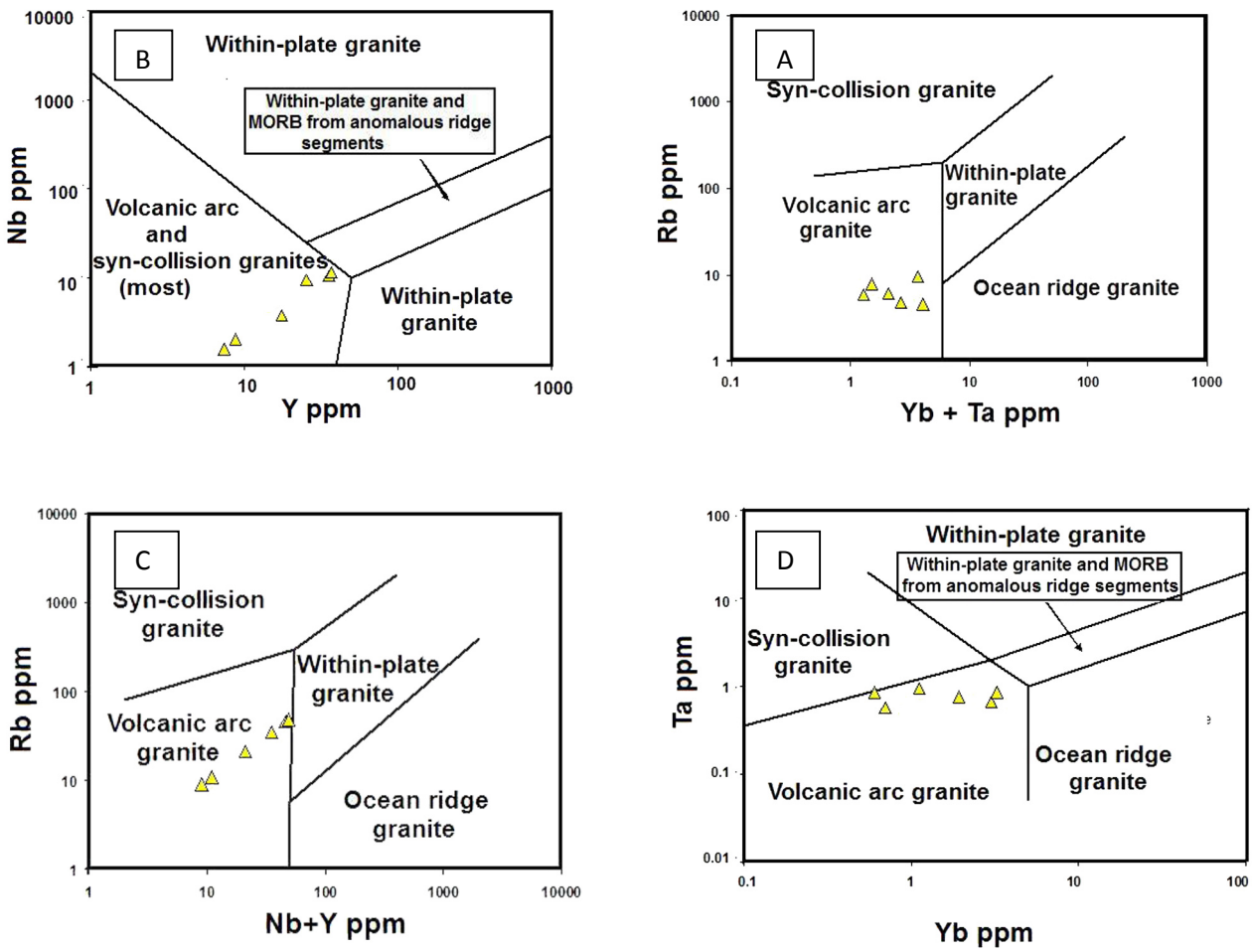

Fig. 7: Plots of the Wadi Rashid Granitoids in the:
A: (Nb vs Y)
B: (Rb vs Yb +Ta)
C: (Rb vs. Nb + Y)
D: Ta vs. Yb discrimination diagrams of (Pearce, *et al*., 1984).

GABBRO

1- Igneous and structural setting

As stated above, the samples from Wadi Rashid composite suite can be divided megascopically, microscopically and geochemically into granitoid and gabbro. Megascopically, the margins of the leucocratic 'granitoid' breccia bodies against the melanocratic gabbroic matrix are medium to fine-grained and the boundaries between them are irregular and lobate. While some of the gabbroic material remained intact, many of the discrete granitoid enclaves are connected by felsic veins throughout the gabbro-granite interfaces. These veins are formed by

break up of semi-consolidated leucocratic 'granitoid' material due to density instabilities in the underlying mafic crystal mush. Contrary to the melanocratic 'gabbroic' rocks, in the leucocratic 'granitoid' rocks magma mingling rather than mixing is more evident. The petrographic study of gabbro–granitoid interfaces shows that as gabbroic magma and peralkaline anatectic melt mix, liquidus crystals (i.e augite, ilmenite and plagioclase) from the gabbroic liquid become partially dissolved and serve as substrates for the nucleation and precipitation of felsic minerals (i.e. albite and anorthoclase) and agpaitic assemblages (i.e. kaersutite and aenigmatite) in the new alkali metaluminous hybrid melt. In addition to partial assimilation of the anatectic grantoid melt, the gabbro shows rhythmic layering (R13 in Fig. 2B). In contrast to the granitoid rocks, Wadi Rashid gabbros have an unusual geochemical signature, which provides evidence for open-system processes and multiple-sources (i.e., assimilation of granitoid anatectic melt and fractional crystallization of the intruded gabbroic magma). Quantitative model describing open-system processes such as assimilation–fractional crystallization (AFC) based on the chondrite-normalized REE diagram of Wadi Rashid gabbros was carried by Al.Sheraefy (2009).However the AFC quantitative model needs further in-situ field and geochemical inspections.

2- Geochemical signature and tectonomagmatic characteristics

The chondrite-normalized REE diagram (Fig. 8) shows the ????Wadi Rashid gabbros have gently sloping patterns that are all moderately light REE-enriched (chondrite-normalized La/Yb = 1.77 to 3.43), have flat heavy REE profiles (chondrite-normalized Tb/Yb = 1.09–1.28) and small negative Eu anomalies (Eu/Eu*= 0.79-0.91). An exception is R13 which has rhythmic layering and is characterized by a small positive Eu anomaly and low heavy REE. In primitive mantle-normalized multi-element diagrams, all samples show depletion in Ba, Pb and Sr relative to adjacent REEs, Ta and Nb negative anomalies and flat Zr to Sm profiles that are similar to those of enriched MORB. The exception is the highly granitoid contaminated R13, which has an unusual Hf-Zr negative anomalies (Fig. 6). The gabbros and grantoids, are characterized by strong negative anomalies in Th, and U (Fig. 8). This lack of enrichment of Th and U in Wadi Rishad gabbro-granitoid suite implies that these elements were mobilized by late-magmatic processes. The contrast between the two rock groups is most remarkable in rare earth elements (REE) and multi-elements spider diagrams (Fig. 6 and 8).

The Hf-Th-Ta, Nb-Zr-Y, Ti-Zr-Y and Ti-Zr-Sr diagrams (Fig. 9) are useful for distinguishing different tectonic settings of gabbros. In these diagrams, Wadi Rishad gabbros show an affinity with E type MORB (Fig. 9).

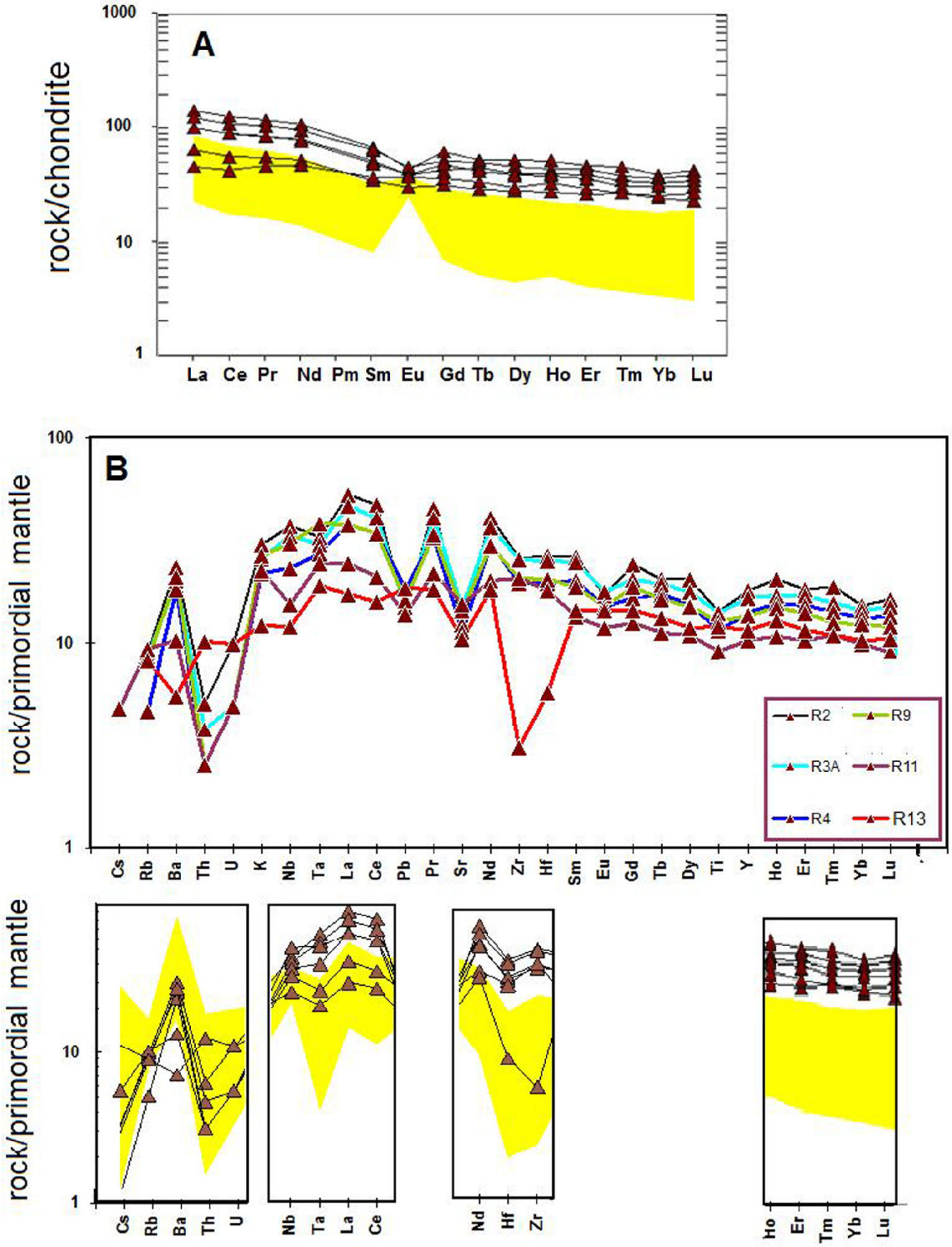

Fig. 8: **A:** Chondrite - Normalized REE Patterns for Gabbroic Samples from Wadi Rashid. Normalization Values from Sun and McDonough (1989).

B: Primitive Mantle - Normalized Incompatible Element Patterns for Samples from Wadi Rashid. Normalization Values from (Wood *et al.*, 1979). The Yellow Shading Shows the Compositional Range of Granitoid Ssamples for Comparison.

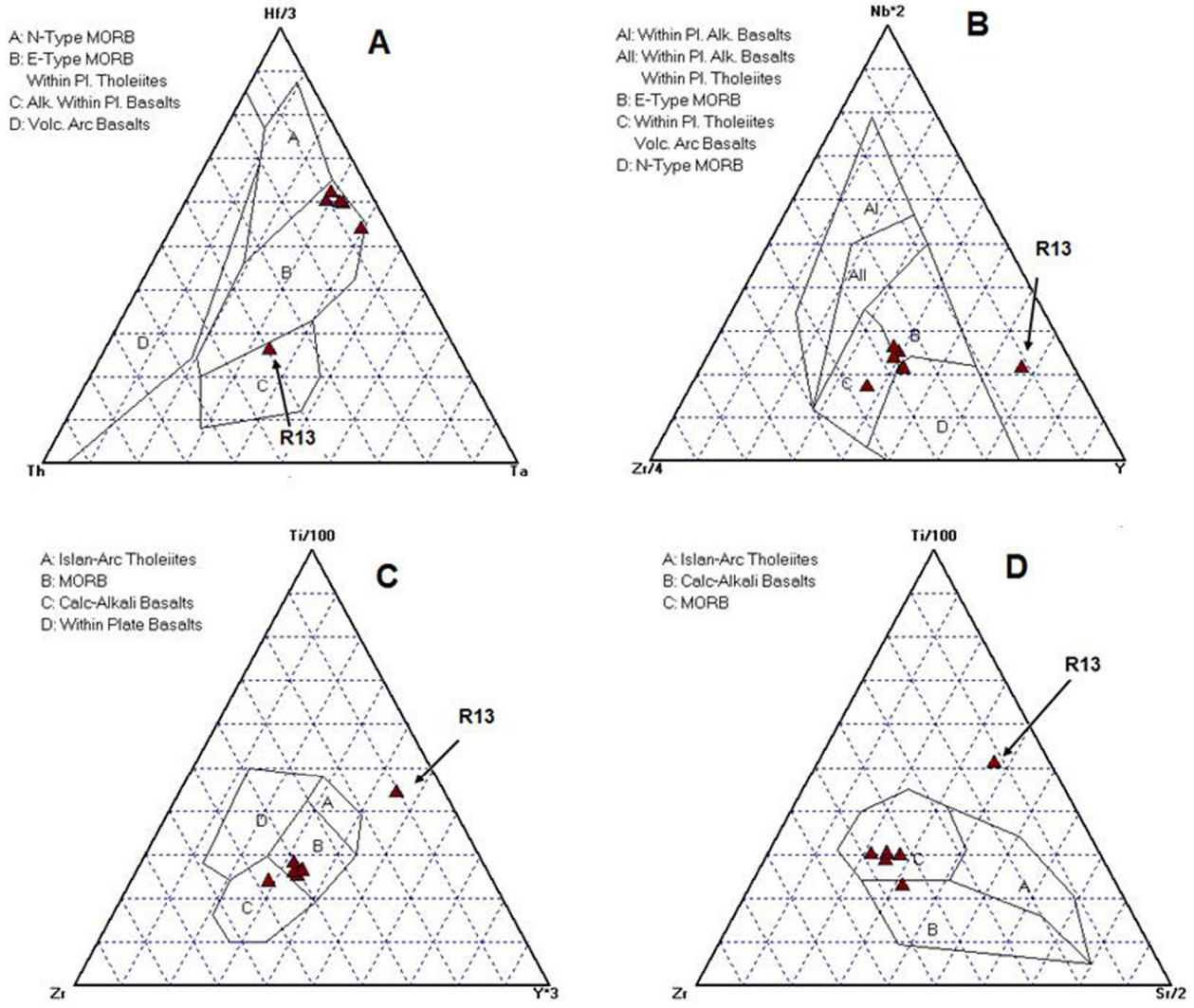

Fig. 9: Tectonic Discrimination Diagrams from:
A: Wood (1980)
B: and **C**- Pearce (1982)
D: Pearce and Cann (1973) Suggesting a EMORB Affinity for the Wadi Rashid Gabbro**.**

DISCUSSION AND CONCLUSIONS

Petrogenesis of the Wadi Rashid granitoid-gabbro suite

A noteworthy aspect of Wadi Rashid granitoid-gabbro suite is the variability of magmatic conditions (i.e. temperature, oxygen fugacity (fO_2) and water fugacity (fH_2O)). The primary 'orthomagmatic' kaersutite equilibrated at a nearly constant pressure of about 269-277 MPa and at crystallization temperatures of between 933-935°C. The logfO_2 during equilibration of kaersutite in the hosting melanosome is in the range of -12.2 to -12.4 (Δlog fO_2 (FMQ) ~ 0.6) and melt water contents slightly higher than 4 wt. %. The amphiboles in the leucosome and contaminated melanosome indicate equilibration at a relatively lower temperature (~753°C) in comparison with that of the melanosome. Ti-rich Fe-biotite-ilmenite and aenigmatite (or titano magnetite) bearing granitoids show fO_2 in log unit deviations from the quartzfayalite- magnetite buffer (Δlog fO_2 (FMQ) spanning fO_2 from FMQ ~ -4 to FMQ ~1). The stability of Ti-rich Fe-biotite, for instance, is at a temperature of 647°C and requires an appreciable amount of H_2O (several wt. % of H_2O) whereas aenigmatite is stable at a maximum temperatures of 753°C under H_2O melt-poor conditions with antipathetic relationships between aenigmatite and Fe-Ti oxides (Di Carlo *et al.,* 2010); as indicated by the reaction relationship:

aenigmatite + O_2= ilmenite +silica+ Nds (sodium disilicate activity).

In addition to T and fO_2 conditions, the aenigmatite crystallization requires melt peralkalinity higher than 12 (e.g. in the form of sodium disilicate) and pressures >100 MPa (Di Carlo *et al.,* 2010). The alkanilinity index of Wadi Rashid granitoid, however, is slightly less than unity. But the megascopic and microscopic observations of Wadi Rashid granitoids verify that peralkaline 'granitoid' anatectic melt could have been produced from a near-metaluminous source (i.e. Wadi Rashid granitoid).

Geochemistry and tectonic Setting of the Wadi Rashid granitoid-gabbro suite

The lack of continuous elemental trends from the gabbros to the granitoids on element-element diagrams indicates that these rocks did not evolve through differentiation of a single basic magma. The granitoid rocks were formed by partial melting of a subducted metabasic precursor where as the low HREE suggests that these elements were compatible during the melting reaction. These data are consistent with melting of a metabasic source in which garnet ± hornblende were residuals. Thus in low-K calcic amphibolite, garnet is a residual phase during amphibole dehydration melting at pressure greater than ~0.7–0.9 GPa (e.g., Wolf and Wyllie, 1994), which is equivalent to a depth of melting of at least 25 km.

Whereas, the E-MORB type geochemical signatures of the relatively younger gabbroic rocks advocate that many of them formed in an extensional tectonic environment, such as an intra-arc rift or a back arc. Hence contrary to the gabbroic rocks at Wadi Rashid that were erupted in an extensional stress regime, the granitoid rocks show a volcanic-arc granitoids (VAG) signatures.

The style of plutonism and the bimodal nature of the studied rocks suggest that igneous activity occurred during crustal extension. (Bickford and Hill, 2007) argued that bimodal igneous suites are characteristic of continental extensional magmatism, whereas (Whitmeyer and Karlstrom, 2007) contend that bimodal magmatism is not unusual in oceanic arcs. In principle, these hypotheses can be tested with geochemical data since arc, rift and back-arc magmatism are generally compositionally distinct in modern environments (e.g., Pearce and Cann, 1973; Pearce and Norry, 1979; Wood, 1980; Pearce and Peate, 1995). Nevertheless, the fact that the relatively younger Wadi Rashid gabbroic rocks have clear EMORB signatures and the granitoid rocks have a volcanic-arc granitoid (VAG) signatures, this suggests that the voluminous gabbro diorite intrusions of Bulfat Complex may reflect granitoid arc magmatism and a subsequent extensional-arc to back-arc basic magmatism around 45 Ma.

Wadi Rashid composite intrusion (Paleogene age) of arc affinity is unequivocally separated from the tectonically similar (Eocene-Oligocene) Walash-Naopurdan arc-backarc complex (Ali *et al.,* 2012), in the same general area but in a structurally lower thrust slice. These coeval Walash-Naopurdan volcanic activities with the multiphase intrusion of the Bulfat Complex verify the presence of a dual subduction-zone system in Iraqi Zagros Zone (Ali *et al.,* 2012).

ACKNOWLEDGEMENTS

Authors would like to thank Brian Jones, Allen Nutman and Solomon Bukman for their constructive comments on the manuscript.

REFERENCES

Al-Sheraefy, R. M., 2009. Petrographic, Geochemical and Tectonic Evidence of Granitoid - Gabbro, Bulfat Complex, Qala Deza / North-East Iraq (M.sc. thesis): University of Mosul, Collage of Sciences, Iraq (In Arabic with English abstract). 179 p.

Ali, S. A. Buckman, S., Aswad, K. J., Jones, B. G., Ismail, S. A. and Nutman, A. P., 2012. Recognition of Late Cretaceous Hasanbag Ophiolite-Arc Rocks in the Kurdistan Region of the Iraqi Zagros Thrust Zone: A missing Link in the Paleogeography of the Closing Neo-Tethys Ocean. The Geological Society of America, Lithosphere doi:10.1130/L207.1.

Ali, S. A., 2012. Geochemistry and Geochronology of Tethyan-Arc Related Lgneous Rocks, NE Iraq (Ph.D. thesi): Wollongong, NSW, Australia, University of Wollongong, 363 p.

Andersen, D. J. and Lindsley, D. H., 1988. Internally Consistent Solution Models for Fe-Mg-Mn-Ti oxides: Fe-Ti oxides. American Mineralogist, Vol. 73, pp. 714-726.

Aoki, K. and Shiba, A. I., 1973. Pyroxene from lherzolites Inclusions from Itinomegata, Japan. Lithos,Vol. 6, pp. 41 - 51.

Ashley, P. M., Franklin, B. J., and Ray, A. S., 1983. Plagiogranites in the Coolac ophiolite suite, New South Wales, Australia Geological Magazine, Vol. 120, pp. 1 - 20.

Aswad, K. J. and Pashdary, M. A. A., 1984. Thermal Metamorphism of Impure Carbonate Xenoliths in the Gabbroic Rock of Bulfat Complex, NE Iraq. Journal Geological Society of Iraq, Vol. 17, pp. 208 - 235.

Aswad, K. J., 1999. Arc-continent Collision in Northeastern Iraq as Evidenced by Mawat and Penjein Ophiolite Complexes. Rafidain Journal of Sciences, Vol. 10, pp. 51 - 61.

Aswad, K. J. A., Aziz, N. R. H., and Koyi, H. A., 2011. Cr-spinel Compositions in Serpentinites and their Implications for the Petrotectonic History of the Zagros Suture Zone, Kurdistan.

Aziz, N. R. H., Aswad, K. J. A., and Koyi, H. A., 2011. Contrasting Settings of Serpentinite Bodies in the Northwestern Zagros Suture Zone, Kurdistan Region, Iraq. Geological Magazine, Vol. 148, pp. 819 - 837.

Barbieri, M., Caggianello A., Di Floris M. R., and Lorenzoni S., 1994. Plagiogranites and Gabbroic Rocks from the Mingora, Ophiolite Mélange, Swat Valley, NW Frontier Province, Pakistan, Mineralogical Magazine, Vol. 58, pp. 553 - 566.

Bard, J. P., 1970. Composition of Hornblendes Formed During the Hercynian Progressive Metamorphism of the Aracene Metamorphic Belt (SW Spain). Contributions to Mineralogy and Petrology, Vol. 28, pp. 117 - 134.

Barker, F., 1979. Trondhjemite: Definition, Environment and Hypotheses of Origin. In Barker, F. (ed.) Trondhjemites, Dacites, and Related Rocks. Elsevier, Amsterdam, pp. 1 - 12.

Beard, J. S. and Lofgren, G. E., 1991. Dehydration Melting and Watersaturated Melting of Basaltic and Andesitic Greenstones and Amphibolites at 1, 3 and 6.9 kb. J. Petrol., Vol. 32, pp. 465 - 501

Bickford, M. E., and Hill, B. M., 2007. Does the Arc accretion Model Adequately Explain the Paleoproterozoic Evolution of Southern Laurentia? An expanded Interpretation: Geology, Vol. 35, pp. 167 - 170.

Blundy, J. D. and Holland, T. J. B., 1990. Calcic Amphibole Equilibria and a New Amphibole-Plagioclase Geothermometer. Contributions to Mineralogy and Petrology, Vol. 104, pp. 208 - 224.

Bonnefoi, C.C, Provost A and Albarede F., 1995. The "Daly gap" as a Magmatic Catastrophe. Nature, Vol. 378, pp. 270 - 272.

Borsi, L., Scharer, U., Gaggero, L., and Crispini, L., 1996. Age, Origin and Geodynamic Significance of Plagiogranites in lherzolites and Gabbros of the Piedmont-Ligurian ocean Basin. Earth and Planetary Science Letters, Vol. 140, pp. 227 - 241. doi:10.1016/0012-821X(96)00034-9.

Buda, GY.,1993. Igneous Petrology of the Bulfat Area (North - East Iraqi Zagros Thrust Zone).

Coleman, R. G. and Donato, M., 1979. Oceanic Plagiogranite Revisited. In Trondhjemites, Dacites and Related Rocks (ed. Barker, F.), Elsevier, Amsterdam, pp. 297 - 300.

Coleman, R.G. and Peterman, Z. E., 1975. Oceanic Plagiogranite. Journal of Geophysical Research, Vol. 80, pp. 1099 - 1108.

Di Carlo I, Rotolo S.G, Scaillet B, Buccheri V. and Pichavant M., 2010. Phase Equilibrium Constraints on pre-eruptive conditions of recent felsic explosive volcanism at Pantelleria Island, Italy. Journal of Petrology, Vol. 51, pp. 2245 - 2276.

Ernst, W. G ; Liu, J., 1998. Experimental Phase-Equilibrium Study of Al- and Ti- Contents of Calcic Amphibole in MORB L. A. Semiquantitative Thermobarometer. American mineralogist, Vol. 83, pp. 952 - 969.

Ferry, J. M. and Spear, F. S., 1978, Experimental calibration of the partitioning of Fe and Mg between Biotite and Garnet. Contributions to Mineralogy and Petrology, Vol. 66, pp. 113 - 117.

Foster, M. D., 1960. Interpretation of the Compositions of Lithium Micas. United States Professional Paper Geological Survey, Vol. 354-E, pp. 115 - 147.

Frost, B. R., Barnes, C. G., Collins, W. J., Arculus, R. J., Ellis, D. J. and Frost, C. D., 2001, A geochemical Classification for Granitic Rocks. Journal of Petrology, Vol. 42, pp. 2033 - 2048.

Gerlach, D. C., Leeman, W.P. and Lallemant, H. A., 1981. Petrology and Geochemistry of Plagiogranite in Canyon Mountain Ophiolite, Oregon. Contributions to Mineralogy and Petrology, Vol. 77, pp. 82 - 92.

Ghiorso, M. S. and Sack, R. O., 1991. Fe-Ti oxide Geothermometry: Thermodynamic Formulation and the Estimation of Intensive Variables in Silicic Magmas. Contributions to Mineralogy and Petrology, Vol. 108, pp. 485 - 510.

Henry, D. J. and Guidotti, C. V., 2002. Ti in Biotite from Metapelitic Rocks: Temperature Effects, Crystallochemical Controls and Petrologic Applications. American Mineralogist, Vol. 87, pp. 375 - 382.

Jassim, S. Z., Suk, M., and Waldhausrova, J., 2006. Magmatism and Metamorphism in the Zagros Suture. In Jassim, S. Z., and Goff, J. C., (eds), Geology of Iraq. Dolin, Prague and Moravian Museum, Brno, pp. 212 - 231.

Jassim, S. Z.,Waldhausrova, J. and Suk, M. 1982. Evolusion of Magmatic Activity in Iraqi Zagros Complexes. Krystalinikum, Vol. 16, pp. 87 - 108.

Jeffery, P.G. and Hutchison, D. 1981. Chemical Methods of Rock Analysis.

Koepke, J., Feig S. T, Snow, J. and Freise, M., 2004. Petrogenesis of Oceanic Oceanic Plagiogranites by Partial melting of Gabbros: an Experimental Study. Contribution to Mineralogy and Petrology, Vol. 146, pp. 414 - 432. doi: 10.1007/s00410-003-0511-9

Kontinen, A., 1987. A early Proterozoic Ophiolite: the Jomua Mafic-Ultramafic Complex, Northern Finland. Precambrian Research , Vol. 35, pp. 313 - 341.

Lattard, D., Sauerzapf, U., Käsemann, M., 2005. New Calibration Datafor the Fe–Ti Oxide Thermo-Oxybarometers from Experiments in the Fe–Ti–O System at 1 Bar, 1000-1300 °C and a Large Range of Oxygen Fugacities. Contribution to Mineralogy and Petrology, Vol. 149, pp. 735 - 754

Leake, BE., Wooley, AR., Arps, CES., Birch, WD., Gilbert, MC., Grice, JD., Hawthrone, FC., Kato, A., Kisch, HJ., Krivovichev, VG., Linthout, K., Laird, J., Mandarino, JA., Maresch, WV., Nickel, EH., Rock, NMS., Schumacher, JC., Smith, DC., Stephensen, NCN., Ungaretti, L., Whittaker, EJW and Youzhi, G., 1997. Nomenclature of Amphiboles: Report of the Subcommitee on Amphiboles of the International Mineralogical Association, Commission on New Minerals and Mineral Names. American Mineralogist, Vol. 82, pp. 1019 - 1037.

Maniar, P. D. and Piccoli, P. M., 1989. Tectonic Discriminations of Granitoids. Geological Society of America Bulletin, Vol. 101, pp. 635 - 643.

McDonough W. F. and Sun S., 1995. “The Composition of the Earth” Chemical Geology, Vol. 120, pp. 223 - 253.

Middlemost, E. A. K., 1985. Naming Materials in the Magma/Igneous Rock System. Earth-Sciences Reviews, Vol. 37, pp. 215 – 224.

Morimoto, N., Fabries, J., Ferguson, A. K., Ginzburg, I.V., Ross, M., Seifert, F. A., Zussman, J., Aoki, K., and Gottardi, G., 1988. Nomenclature of Pyroxenes. Mineralogical Magazine, Vol. 52, pp. 535 - 550.

Nair, R. and Chacko, T., 2008, The Role of Oceanic Plateaus in Subduction Initiation and Origin of Continental Crust. Geology, Vol. 36, pp. 583 - 586.

Nicholls, J., and Carmichael, I. S. E., 1969. Peralkaline Acid liquids: a Petrological Study. Contributions to Mineralogy and Petrology, Vol. 26, pp. 268 - 294.

Nimis, P., 1995. A clinopyroxene Geobarometer for Basaltic Systems Based on Crystal-Structure Modeling. Contributions to Mineralogy and Petrology, Vol. 121, pp. 115 - 125.

Nisbet, E. G., and Pearce, J. A., 1977. Clinopyroxene Composition in Mafic Lavas from Different Tectonic Settings. Contributions to Mineralogy and Petrology, Vol. 63, pp. 149 - 160.

Pearce, J. A. and Parkinson, I. J., 1993. Trace Element Models for Mantle Melting: Application to Volcanic Arc Petrogenesis. In: Prichard, H. M., Alabaster, T., Harris, N. B. W. and Neary, C. R. (Editors). Magmatic

Processes and Plate Tectonics. Geological Society, London, Special Publications, Vol. 76, pp. 373 - 403.

Pearce, J. A., Harris, N. W. and Tindle, A. G., 1984. Trace Element Discrimination Diagrams for the TectonicIinterpretation of Granitic Rocks. Journal of Petrology, Vol. 25, pp. 956 - 983.

Pearce, J.A., and Cann, J.R., 1973. Tectonic Setting of Basic Volcanic Rocks Determined using Trace Element Analyses: Earth and Planetary Science Letters, Vol. 19, pp. 290 - 300.

Pearce, J. A., and Norry, M. J., 1979. Petrogenetic Implications of Ti, Zr, Y, and Nb Variations in Volcanic Rocks: Contributions to Mineralogy and Petrology, Vol. 69, pp. 33 - 47.

Pearce, J.A., and Peate, D.W., 1995. Tectonic Implications of the Composition of Volcanic arc Magmas: Annual Review of Earth and Planetary Sciences, Vol. 23, pp. 251 - 285.

Pergamon Press: Oxford, United Kingdom. Raase, P., 1974. Al and Ti Contents of Hornblende, Indicators of Pressure and Temperature of Regional Metamorphism. Contributions to Mineralogy and Petrology, Vol. 45, pp. 231 - 236.

Rapp, R. P., Watson, E. B., Miller, C. F., 1991. Partial Melting of Amphibolites /Eclogite and the Origin of Archaean Trondhjemites and Tonalites. Precambrian Research, Vol. 51, pp. 1 - 25.

Region, Iraq: Geological Magazine, Vol. 148, pp. 802 - 818, doi: 10.1017 / S0016756811000422.

Ridolfi, F., Renzulli, A. and Puerini M., 2010. Stability and Chemical Equilibrium of Amphibole in Calc-Alkaline Magmas: an Overview, New Thermobarometric Formulations and Application to Subduction-Related Volcanoes. Contribution to Mineralogy and Petrology, Vol. 160, pp. 45 - 66.

Rushmer, T., 1991. Partial Melting of Two Amphibolites: Contrasting Experimental Results Under Fluid-Absent Conditions. Contributions to Mineralogy and Petrology, Vol. 107, pp. 41 - 59.

Sepp, B. and Kunzmann, T., 2001, "The stability of Clinopyroxene in the System CaO-MgO-SiO_2-TiO_2(CMST)", American Mineralogist, Vol. 86, pp. 265 - 270.

Stuckless, J. S., Bunker, C. M., Bush, C. A., Doering, W. P., and Scott, J. H., 1977. Geochemical and Petrological Studies of a Uraniferous Granite from the Granite Mountains, Wyoming: U. S. Geological Survey Journal of Research, Vol. 5, pp. 61 - 81.

Sun, S. S., and McDonough, W. F., 1989. Chemical and Isotopic Systematics of Oceanic Basalts: Implications for Mantle Composition and Processes, in Saunders, A. D., and Norry, M. J., (editors), Magmatism in the Ocean Basins: Geological Society of London Special Publication, Vol. 42, pp. 313 - 345.

Wass, S. Y., 1979. Multiple Origins of Clinopyroxenes in Alkalic Basaltic Rocks. Lithos, Vol. 12, pp. 115 - 132.

Weaver S. D., 1977. The Quaternary Caldera Volcano Emuruangogolak, Kenya Rift, and the Petrology of a Bimodal Ferrobasalt-Pantelleritic Trachyte Association. Bulletin of Volcanology, Vol. 40, pp. 209 - 230.

Whitmeyer, S. J., and Karlstrom, K. E., 2007. Tectonic Model for the Proterozoic Growth of North America: Geosphere, Vol. 3, pp. 220 - 259.

Wilson, M., 1989. Igneous Petrogenesis. Springer, 466 p.

Wolf, M. B., and Wyllie, P. J., 1994. Dehydrationmelting of Amphibolite at 10 kbar: The Effects of Temperature and Time: Contributions to Mineralogy and Petrology, Vol. 115, pp. 369 - 383.

Wones, D. R. and Eugster, H. P., 1965. Stability of Biotite: Experiment, Theory, and Application. American Mineralogist, Vol. 50, pp. 1228 - 1272.

Wood, D.A., Joron, J. L., and Treuil, M. ,1979. A re-Appraisal of the Use of Trace Elements to Classify and Discriminate between Magma Series Erupted in Different Tectonic Settings. Earth Planet. Sci. Letts. Vol. 45, pp. 326 - 336.

Wood, D.A., 1980. The Application of a Th-Hf-Ta Diagram to Problems of Tectonomagmatic Classification and to Establishing the Nature of Crustal Contamination of Basaltic Lavas of the British Tertiary Volcanic Province: Earth and Planetary Science Letters,Vol. 50, pp. 11 - 30.

Yagi, K. and K. Onuma, 1967. The Join $CaMgSi_20_6$-$CaTiAl_2O_6$ and its Bearing on the Titanaugites. Journal of the Faculty of Science, Hokkaido University, Vol. 13, pp. 463 - 483.